The Pennsylvania State University
The Graduate School

MOLECULAR DYNAMICS SIMULATIONS FOR ELECTROMAGNETIC PROPULSION OF NON-IONIZED WATER MOLECULES

A Thesis in
Aerospace Engineering
by
Shivani H. Sodawala

Submitted in Partial Fulfillment
of the Requirements
for the Degree of

Master of Science

August 2018

The thesis of Shivani H. Sodawala was reviewed and approved* by the following:

Michael M. Micci
Professor of Aerospace Engineering
Thesis Advisor

Sven G. Bilén
Professor of Engineering Design, Electrical Engineering, and Aerospace Engineering
Reader

Jack W. Langelaan
Associate Professor of Aerospace Engineering
Director of Graduate Studies

*Signatures are on file in the Graduate School.

Abstract

Use of the Abraham force as a means of electromagnetic propulsion is investigated. Abraham force is exerted by a varying electric field in one direction and a magnetic field in the perpendicular direction, causing an acceleration of a dipole in the third orthogonal direction. Because of their high naturally occurring dipole moment, water molecules are used as propellant. This technique eliminates the need to ionize the propellant, which means this electric propulsion technique is highly energy efficient. Successful molecular dynamics simulations are carried out for single and multiple molecules with random initial orientations and velocities. The molecular dynamics simulations are extended to multiple electric pulses and varying electric field strengths and frequencies to study its effect on acceleration. A z acceleration of 1.979×10^{10} m/s^2 is achieved for 120 water molecules in a 25 T magnetic field in the y-direction and 40 sinusoidal electric pulses of 100,000 V/m at a frequency of 75 GHz in the x-direction. This makes the use of the Abraham force a viable electromagnetic propulsion concept with comparable acceleration to current electric propulsion techniques using ionized propellants.

Table of Contents

List of Figures

List of Tables

List of Symbols

∇	Nabla operator
α	Polarizability; parameter of Wolf method
$\vec{B}$	Magnetic field strength vector [T]
c	Velocity of light [299,792 m/s]
d	Dipole charge separation [m]
$\vec{E}$	Electric field strength vector [V/m]
erfc	Complimentary error function
F	Force [N]
$\vec{H}$	Magnetic field strength vector [A/m]
g	Gravitational acceleration [9.81 m/s^2]
$H1_x$	Position of hydrogen 1 in x direction
$H1_y$	Position of hydrogen 1 in y direction
$H1_z$	Position of hydrogen 1 in z direction
$H2_x$	Position of hydrogen 2 in x direction
$H2_y$	Position of hydrogen 2 in y direction
$H2_z$	Position of hydrogen 2 in z direction
I_{sp}	Specific impulse [s]
m	Mass [kg]
M_{P}	Mass of propellant [kg]
O_x	Position of oxygen in x direction
O_y	Position of oxygen in y direction

O_z	Position of oxygen in z direction
$\vec{P}$	Polarization density [C/m^2]
p	Dipole moment [C·m], Mass-weighted momentum [m/s]
q	Charge of particle [C]
R	Effective radius [m]
r	Position/separation [m]
r_c	Cut-off radius [m]
t	Time [s]
τ	Thrust [N]
u_eq	Exhaust velocity [m/s]
μ_0	Permeability of free space [H/m]
μ_r	Relative permeability [H/m]
V_e	Exit velocity [m/s]
$\vec{V}$	Velocity of charge [m/s]
ϵ	Lennard-Jones potential well depth [N/m]
ϵ_r	Relative permittivity [F/m]
ω	Angular frequency [rad/s]
σ	Lennard-Jones zero energy separation distance [m]
η	Thruster efficiency
ζ	Ionization energy [eV]

Acknowledgments

I would first like to thank my thesis advisor Dr. Michael Micci of the Aerospace Engineering department at The Pennsylvania State University. Dr. Micci was always available whenever I ran into a trouble spot or had a question about my research or writing. He consistently allowed this thesis to be my own work, but steered me in the right direction whenever he thought I needed it.

I would also like to acknowledge Dr. Bilén of the Electrical Engineering and Aerospace Engineering Departments being the reader of this thesis, and I am gratefully indebted to him for his valuable time and comments on this thesis. I also appreciate the time of Dr. Pritchett, department head of Aerospace Engineering and Dr. Jack Langelaan, Professor of Aerospace Engineering, for reviewing my work.

A big thanks to the IT specialists of the Aerospace department, Kirk Heller and Ben Enders, for their prompt responses and help with any technical problems concerning the computing clusters or programming queries regarding the message passing interface (MPI).

A huge thanks to Jeffrey Contri, a fellow researcher of the Aerospace Engineering department for getting me up to speed with this research and helping me along the path.

Finally, I must express my very profound gratitude to my parents, my grandparents, and to my sister Chandni for providing me with unfailing support and continuous encouragement throughout my years of study and through the process of researching and writing this thesis. Last but not the least, this accomplishment would not have been possible without constant support of my friends Amrit, Milan and Saman. Thank you.

Chapter 1

Introduction

Propulsion is the force that accelerates a vehicle. Space vehicles with a requirement to travel the largest distance and/or at the greatest speed require much focus on their propulsion systems. A propulsion system comprises of a means to "burn" fuel and convert the energy into kinetic energy to produce the desired thrust. The two types of rocket propulsion are chemical propulsion and electric propulsion. The names suggest the fundamental technique of generating thrust. The thrust in a chemical propulsion system is produced as a result of a chemical reaction. The propellant is burned or oxidized in the chamber followed by a nozzle expansion generating thrust. Whereas electric propulsion systems use electric and/or magnetic fields to accelerate the charged particles to generate thrust.

Chemical propulsion has been used since the beginning days of rocket propulsion. The fuel is usually burned or oxidized to produce the required kinetic energy. Thus, the energy available is limited to the energy stored in the mass of the propellant. As advances were made in space science during the 1950s, the payload mass that needed to be propelled increased. This was seen as a limitation of the chemical propulsion techniques available at that time. Electric propulsion techniques were advocated as the energy required for propulsion was no longer constrained by the propellant [1]. The energy for electric propulsion was provided by solar or nuclear means. Although electric propulsion was discovered in the early 1900s, the first experimental flights flew in the 1960s by the US and Russia. By 1990s, electric propulsion was more deeply rooted as a propulsion technique. Electric and chemical propulsion techniques were compared on the basis of specific mass, exhaust velocity, mass flow rate, and thrust. Electric propulsion succeeded in generating higher exhaust velocities for lower mass of the propellant. That was an important achievement required to accelerate the increasing payloads.

Many current and future missions rely on electric propulsion techniques. Understanding the existing methods of electric propulsion is crucial for situation of this research. Electric propulsion is comprised of three basic categories:

1. Electrothermal thrusters

2. Electrostatic thrusters

3. Electromagnetic thrusters

In electrothermal thrusters, electric energy is used to heat the propellant followed by a nozzle expansion. Electrothermal thrusters use different types of electrical energy like microwaves, plasma and lasers to heat the propellant. The kinetic energy is then obtained by nozzle expansion of the propellant similar to chemical thrusters hence, is the closest variant of electric thruster to chemical propulsion. A few examples are resistojets, arcjets, microwave heated thrusters and laser heated thrusters.

Electrostatic thrusters use steady electric fields to accelerate a propellant that is previously ionized. Well-known examples of electrostatic thrusters are ion thrusters and hall thrusters. Figure 1.1 shows the schematic of an ion thruster. A neutral propellant, for example xenon, enters the ionizer where it is ionized. The positive ions are then accelerated due to an electric field $\vec{E}$ generated as a result of an applied potential ΔV between two grids. The electrons are later added to the exhaust stream. Hall thrusters and ion thrusters have proved their capabilities through a large number of missions during the past two decades. For any future deep space exploration like the Mars mission, these types of electric propulsion methods provide great hope [2].

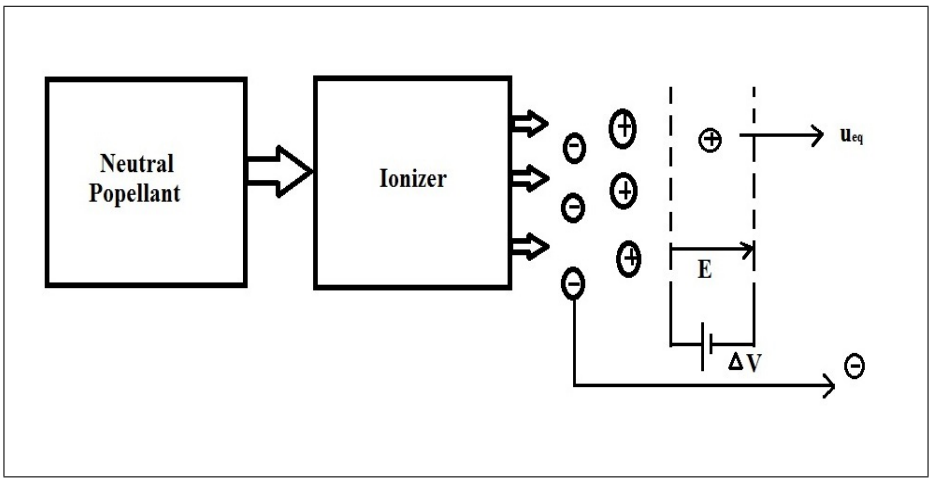

Figure 1.1. Schematics of an electrostatic ion thruster

Thrust mechanism of an electromagnetic thruster is a combination of steady or unsteady electric fields and magnetic fields used to accelerate an ionized propellant. Figure 1.2 shows the schematic of an electromagnetic thruster. The role of the ionizer is the same as in an electrostatic thruster, that is, to ionize a neutral propellant. But the charged particles are accelerated in the presence of perpendicularly oriented electric and magnetic fields. The Lorentz force accelerates the charged particles in the third orthogonal direction. The figure shows an electric field in y direction, magnetic field in z direction, and the propellant being accelerated in the x direction. Example of a electromagnetic thruster will be magnetoplasmadynamic thruster (MPD).

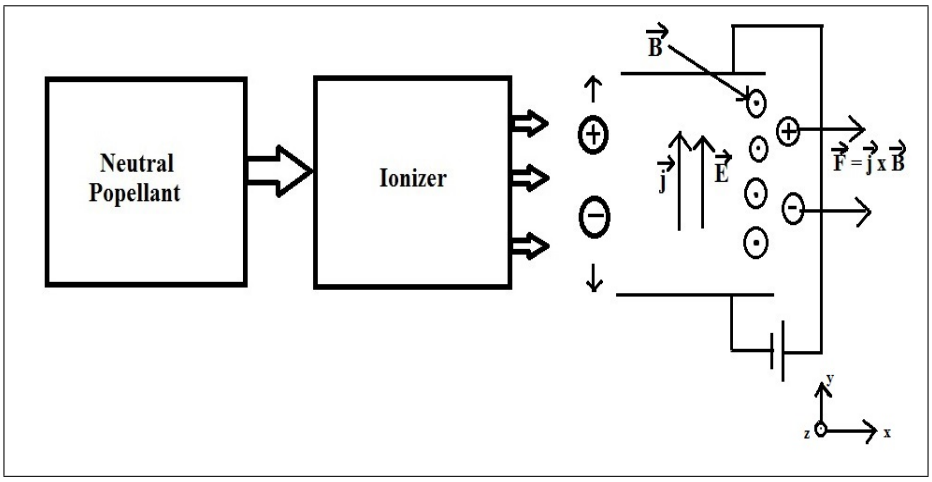

Figure 1.2. Schematics of an electromagnetic thruster

Compared to chemical propulsion techniques, electrical propulsion gave the advantage of high exhaust velocities and thus high specific impulses. Specific impulse is the ratio of the thrust produced to the mass flow rate of the propellant,

$$I_{\mathrm{sp}} = \frac{\tau}{M_{\mathrm{p}} g}. \tag{1.1}$$

The thrust, assuming the effect of the exterior pressure is negligible, is given by

$$\tau = M_{\mathrm{p}} u_{\mathrm{eq}}. \tag{1.2}$$

Therefore, the I_{sp} can be written as

$$I_{\mathrm{sp}} = \frac{u_{\mathrm{eq}}}{g}, \tag{1.3}$$

which means specific impulse is directly proportional to the propellant's exit velocity. The specific impulse for electric propulsion starts from around 1000 s (except microwave electrothermal thruster), whereas it is close to a few 100 s for chemical propulsion. Higher specific impulses in the electric propulsion system, therefore, mean higher exhaust velocities, but lower mass flow rates of the propellant giving much lower thrust compared to chemical propulsion.

Even though electric propulsion is under consideration for future space exploration, it has a limitation of low efficiency at low specific impulses. Lower efficiency gives an indication of power wastage in the system. Only a part of the input power is converted into output power. While lower efficiency does not hamper the operation of the system, it means that it requires more power to generate the desired thrust. A larger power requirement in the case of space propulsion can mean more mass of the power source on board. Thus, electric propulsion is more beneficial over chemical propulsion by its higher exhaust velocities, but it comes at the cost of lower efficiency. This research is focused on describing on electric propulsion technique that is more energy efficient.

1.1 Motivation

Current electric propulsion techniques have many advantages over chemical propulsion, but they are plagued with low efficiency. This section presents the proof for and explains the need for a new method. Power for a propulsion system is given by

$$P = \frac{\tau u_{\text{eq}}}{2\eta}. \tag{1.4}$$

It is proportional to the product of the thrust and exhaust velocity. Electric propulsion techniques have the characteristic of higher specific impulses and exhaust velocities, but low thrust values.

Performance of a system can be best gauged by its efficiency. The efficiency of an electric propulsion system can be defined as the ratio of the beam power to the total input power, which is the sum of the beam power and various loss mechanisms, i.e.,

$$\eta_{\text{T}} = \frac{P_{\text{Beam}}}{P_{\text{Total}}}, \tag{1.5}$$

where

$$P_{\text{Total}} = P_{\text{Beam}} + P_{\text{Losses}}. \tag{1.6}$$

Beam power is the energy that gets converted into kinetic energy of the propellant. Thus we can also write the efficiency as

$$\eta = \frac{\frac{mu_{\text{eq}}}{2}}{\frac{mu_{\text{eq}}}{2} + P_{\text{Losses}}}. \tag{1.7}$$

These loss mechanisms involve, but are not limited to, energy used for ionizing the propellant, ion recombination effects, boundary absorption, and radiation effects. Ionization energy is considered the primary loss mechanism in electrostatic and electromagnetic thrusters.

For both an electrostatic and electromagnetic thruster, once the propellant exits the system, the energy used in ionization cannot be recovered. Also, there is a need to neutralize the expelled charged particles so that the spacecraft does not accumulate charge and cause beam stalling. So, there is energy being invested in ionizing the propellant, which at the end of the process needs to be deionized again. This is why, ionization energy is considered as the primary loss mechanism for such thrusters.

Single ionization energies for commonly used propellants like lithium, argon, xenon, and cesium fall in the range of 3.89–15.75 eV [3]. Due to recombination and radiation effects, the ionization energy of the propellant being used is one-to-two orders of magnitude above the single ionization energy. For reference, consider the NASA Solar Technology Application Readiness (NSTAR) mission, an ion thruster propelled system using xenon as propellant launched in 1998. The ionization energy required by NSTAR was approximately 240 times the single ionization energy of xenon [13]. This makes ionization energy the primary loss mechanism. The numbers for efficiency of the current systems with the most common propellants is shown in Figure 1.3. A plot of efficiency versus specific impulse is shown for some of the frequently used propellants. The

ion production energy is assumed to be ten times the single ionization energy and is considered as the only loss mechanism for the thruster. The efficiency is given by

$$\eta = \frac{\frac{mu_{\text{eq}}^2}{2}}{\frac{mu_{\text{eq}}^2}{2} + 10\zeta}, \tag{1.8}$$

where ζ is the single ionization energy and the beam power is considered to be the gain in kinetic energy of the propellant, i.e.,

$$P_{\text{Beam}} = \frac{mu_{\text{eq}}^2}{2}. \tag{1.9}$$

In the presented plot, efficiency is increasing with the specific impulse because the ion production energy becomes a lower fraction of the total thruster energy input as the exhaust kinetic energy increases. In other words, $P_{\text{Ionization}}$ becomes a lower fraction of P_{Total} as P_{Beam} keeps increasing, which makes the P_{Losses} lower and increases the overall efficiency. But, the efficiency at lower specific impulses is barely 50%. This is also the primary reason that electric thrusters are not able to operate efficiently at low specific impulses.

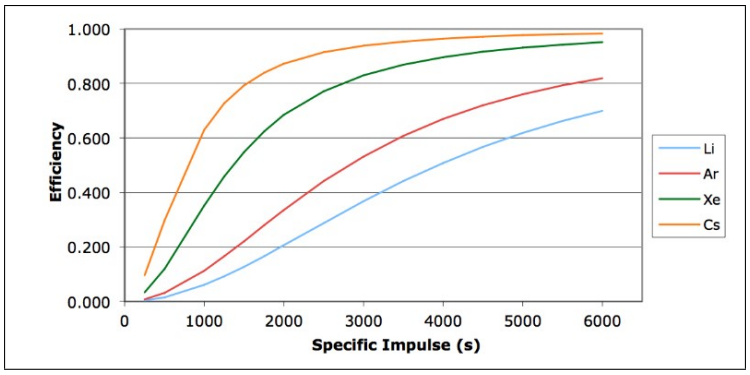

Figure 1.3. Electric thruster efficiency as a function of specific impulse where the only loss is ionization energy [17].

It is evident from the above discussion that revolutionary gains in the thruster efficiency are possible if the need to ionize the propellant is eliminated. Dipole propulsion method is suggested in this research with the same aim. A naturally occurring dipole can be accelerated by the Abraham force through the application of a varying electric field in one direction and varying magnetic field in the perpendicular direction. The Abraham force accelerates the dipole in the third orthogonal direction. Any gas with high dipole moment to mass ratio can be used as a propellant. As the propellant in dipole propulsion is accelerated by the Abraham force which is generated by perpendicularly acting varying electric and magnetic fields, it falls into the category of electromagnetic propulsion. The low efficiency of the current electric thrusters at low specific impulses, visible in Figure 1.3, was the driving force for the research in dipole propulsion. By eliminating the ionizer from electrostatic and electromagnetic thrusters, higher efficiency can be achieved even at low specific impulses.

1.2 Literature Review

In 1909, Abraham was trying to establish a definite system of equations for electrodynamics of moving bodies [4]. He came across an error in the different existing theories and combined them together by adding a new force density term in the force equation. In 1967, Penfield and Haus started deriving a model of a dipolar fluid in their book [6]. Surprisingly, the force which they obtained was similar to what Abraham had derived. Thus, two proofs for the Abraham force are available in the literature.

In 1975, Walker et al. set to measure the Abraham force [7]. The Abraham force, which was only in the form of derivations in literature yet, was measured on a barium titanate specimen by Walker et al. and Walker and Walker [8]. They found a force, but only due to a part of the term which Abraham had added in the electrodynamics of moving body. They called that force, represented by that term, as the Abraham force. The Abraham force obtained was directly proportional to the rate of change of the dipole moment and the magnetic field strength.

Cox suggested the concept of using the Abraham force as a electromagnetic propulsion technique [9][10]. He visualized a dipole subjected to perpendicularly acting varying electric and magnetic fields and derived the force on both the positive and negative ends of the dipole. On addition, he obtained a force which was directly proportional to dipole moment, frequency and magnetic field strength. With the help of his derivations, Cox successfully demonstrated a dipole propulsion concept. On application of varying x directional magnetic field and y directional electric field, the dipole accelerated in the z direction. This was the first successful demonstration of an electromagnetic propulsion method using non-ionized propellant. he suggested some possible propellants with high dipole moment-to-mass ratio and water was one of them. Yet, this was just the beginning for dipole propulsion research. In the 1980s though, both Cox and Micci [12] raised concerns about technologies to generate high frequency varying magnetic field and thus, the research of dipole propulsion was termed as not feasible.

In 2009, Paunescu did molecular dynamics simulations and experiment on the subject of dipole propulsion [13]. To cope with the difficulties of generating high strength and frequency magnetic fields, he did the molecular dynamics simulations with a steady magnetic field. First, he validated the concept by computer simulations in which he obtained an acceleration of 4.96×10^6 m/s^2 by using water as a propellant at 20 kV pulsed electric field and 25 T steady magnetic field. This results encouraged him to perform an experiment in dipole propulsion. Detailed description along with his experimental setup is shown in Section 2.2. Unfortunately, Paunescu's experiment did not indicate any acceleration of the water vapor propellant at that time Thus, there was still some scope of molecular dynamics simulations left.

Contri furthered the molecular dynamics simulations in dipole propulsion [14]. He worked on obtaining the correct initial orientation of water molecule for maximum acceleration. Also, simulations with single water molecule were not being able to replicate a real experiment scenario. Contri therefore extended the molecular dynamics simulations to 1000 water molecules. Three intermolecular forces as the Lorentz force, Coulomb's force, and Lennard-Jones force were cal-

culated between the water molecules and atoms. This system of molecular dynamics simulation was much closer to experimentation than the one before.

This research on dipole propulsion is done using Contri's molecular dynamics simulation system of 1000 water molecules with the aim to find the optimum conditions that give the acceleration comparable with current electric propulsion techniques. If dipole propulsion is established as a viable concept, it can mean very high efficiency thrusters with water as the propellant enabling deep space exploration. Also, due to the abundant availability of water in the solar system, travelling farther than ever before could be made feasible.

Molecular dynamics simulations on the subject of dipole propulsion are explained in this research. There was still a lot of scope for simulations with multiple-molecule model before performing an experiment. There still remains the difficulty of generating very high strength steady magnetic field used for the simulations. Also, an orthogonal high strength and high frequency electric field needs to be applied while monitoring its pulse numbers. Therefore, the right direction to proceed was multiple-molecule simulations for calculating the acceleration by dipole propulsion. Chapter 2 gives a thorough theoretical background in dipole propulsion. All the works by different researchers, introduced in the literature review Section 1.2, are explained in detail. The progress on the subject of dipole propulsion so far with the motivation for this research is made clear. As mentioned before, the research presented uses molecular dynamics to simulate the Abraham force on the propellant molecules which is introduced in detail in Chapter 3. Choice of the parameters for the simulations, along with the various forces calculated between the molecules are described. The final goal of the research is to calculate the acceleration of the water molecules by dipole propulsion and compare it with current electric propulsion techniques. Chapter 4 highlights the results of the research in the form of polarity and acceleration plots. Polarity plots show the movement and alignment of the water molecules in presence of electric and magnetic fields and acceleration plots show the z direction acceleration obtained by changing the various simulations parameters. In conclusion, Chapter 5 presents all the results obtained from this research, its importance and future scope.

Chapter 2

Theoretical Background

In the early 1900s, Abraham put together the work of various scientists and established a system of equations for electrodynamics of moving bodies. Abraham's derivation was then independently verified by others. The force derived was measured experimentally and the existence of the Abraham force was verified. Using the Abraham force for electromagnetic propulsion was suggested by Cox in the 1980s. The concept was then lost for a few decades due to the state of the necessary technologies until the late 2000s when successful simulations were carried out and the research on electromagnetic propulsion with a non-ionized propellant was revived.

2.1 The Abraham Force

In 1909, scientist Max Abraham published papers discussing the electrodynamics of a moving body. His paper [4], translated into English by Delphenich [5], extensively compares all the basic theories of electrodynamics developed at the time by scientists like Hertz, Lorentz, Cohn, and Minkowski. As Abraham noted, the goal of his paper was to find a definitive system of electrodynamics for a moving body that is free from the limitations of other theories [5]. He explained the energy and the impulse equations in order to better analyze the system. According to him, the force acting upon a unit volume of moving matter as a result of the electromagnetic process that an observer will measure will be

$$\begin{aligned} f_x &= \frac{\partial X_x}{\partial x} + \frac{\partial X_y}{\partial y} + \frac{\partial X_z}{\partial z} - \frac{\partial g_x}{\partial t}, \\ f_y &= \frac{\partial Y_x}{\partial x} + \frac{\partial Y_y}{\partial y} + \frac{\partial Y_z}{\partial z} - \frac{\partial g_y}{\partial t}, \text{ and} \\ f_z &= \frac{\partial Z_x}{\partial x} + \frac{\partial Z_y}{\partial y} + \frac{\partial Z_z}{\partial z} - \frac{\partial g_z}{\partial t}, \end{aligned} \tag{2.1}$$

where x,y,z,t are Cartesian coordinates and time, respectively, and the vector g is known as the impulse density. The equation can be known as the impulse equation. He wrote the energy equation as

$$fd + Q = -\nabla.E - \frac{\partial \Psi}{\partial t}, \tag{2.2}$$

where Q is the heat in joules, E is the energy current, and Ψ is the electromagnetic energy density. Energy and impulse equations were the two main equations of the electrodynamics of moving bodies. After scrutinizing the work by all the above mentioned scientists on elecrodynamics of moving bodies, Abraham concluded that an additional term for the force density must be added to the existing theory. Abraham's equation for force is hence,

$$f = \frac{\epsilon_r \mu_r - 1}{c^2} \frac{d(\vec{E} \times \vec{H})}{dt}. \tag{2.3}$$

In 1967, Penfield and Haus independently derived the same force in their book *Electrodynamics of Moving Media* [6]. While discussing the breaking of complete closed systems into a set of open systems, such that they follow the laws of conservation of momentum and energy, Penfield and Haus presented simple physical models for various systems. The derivation of the model of a dipolar fluid lead to the net force F on the dipole in an electromagnetic field,

$$\vec{F} = qd\nabla\vec{E} + q\vec{v} \times (d\nabla)\mu_0\vec{H} + q\frac{d\vec{d}}{dt} \times \mu_0\vec{H}. \tag{2.4}$$

In the force in Equation 2.4, the terms can be combined to form the force density term Abraham described in 1909. Thus, their work produced the same result as Abraham's work.

In 1975, Walker et al. experimentally verified the existence of the Abraham force by measuring the force on a barium titanate specimen. The experiment was performed at a frequency of approximately 0.3 Hz and was restricted to the special case of a time varying electric and a fixed magnetic field in a nonmagnetic dielectric. They suspended a disc of barium titanate as a torsional pendulum and measured the movement of the disk by optical means. By looking at the results, the three scientists unanimously concluded that the measured torque falls within 4% of Penfield and Haus's derivation. Walker and Walker [7] and Walker et al. [8] while searching for the force

$$\vec{F} = q\frac{d\vec{d}}{dt} \times \vec{B} + q\vec{d} \times \frac{d\vec{B}}{dt} \tag{2.5}$$

found only the force due to the first term, known as the Abraham Force, given by

$$\vec{F} = \frac{d\vec{P}}{dt} \times \vec{B}, \tag{2.6}$$

where

$$\vec{P} = q\vec{d}. \tag{2.7}$$

Therefore, even though they showed that Abraham's derivation was in error, they proved that the force derived exists and can be experimentally measured.

The idea of using the force field for propulsion was suggested by Cox in 1980 [9] and 1981 [10]. Cox explained that, when an alternating electric field is applied to a polarized or polarizable material, the dipole can be made to rotate at high frequency and if an alternating and synchronized magnetic field is then applied at preferably right angles to the electric field, a Lorentz force

given by

$$\vec{F} = q(\vec{V} \times \vec{B}) \tag{2.8}$$

is generated, which can accelerate the dielectric fluid in a direction perpendicular to $\vec{B}$ and $\vec{v}$ [9, 10, 11]. Figure 2.1 explains the phenomenon. The dipole is shown with the positive end at the origin and the negative end in the x-z plane. There is an alternating electric field acting in the y direction and an alternating magnetic field in the x direction. The dipole is shown to have a velocity in the z direction. The derivation of the force by Cox is presented here. In the presence

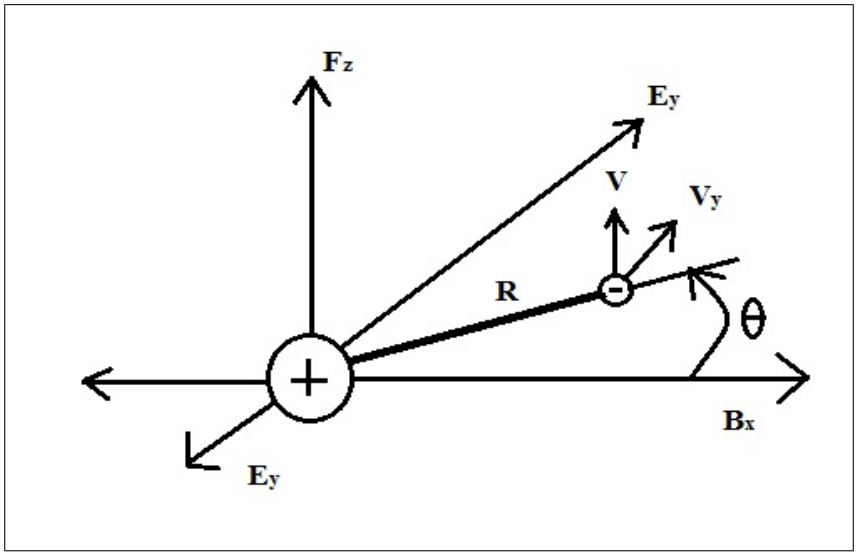

Figure 2.1. Forces on dipole in alternating Lorentz field [9]

of an intense electric field below a molecule's breakdown voltage, a molecule with a permanent dipole moment

$$P_{\mathrm{p}} = qd \tag{2.9}$$

will experience a total polarization

$$P = P_{\mathrm{p}} + P_{\mathrm{i}}, \tag{2.10}$$

where P_{i} is the induced polarization due to the electric field and it is given by

$$P_{\mathrm{i}} = \alpha E, \tag{2.11}$$

where α is the polarizability factor. Now, if the applied electric field is alternating, and an alternating magnetic field is applied at right angles to it, the Lorentz force becomes

$$F = qV_y B_x, \tag{2.12}$$

where

$$V_y = \omega R \cos(\omega t) \tag{2.13}$$

and

$$B_x = B_0 \cos(\omega t). \tag{2.14}$$

This gives the force acting on the positive charge as

$$F_z^+ = q\omega R \cos(\omega t) B_0 \cos(\omega t) \tag{2.15}$$

and on the negative charge

$$F_z^- = -q\omega(-R) \cos(\omega t) B_0 \cos(\omega t). \tag{2.16}$$

The total force is the summation of both forces, i.e.,

$$F = 2q\omega R B_0 \cos^2(\omega t), \tag{2.17}$$

which can be written as

$$F = \omega P_\mathrm{p} B_0 \cos^2(\omega t) \tag{2.18}$$

because P_p is the polarity and

$$P_\mathrm{p} = 2qR. \tag{2.19}$$

Taking the average value of the force,

$$F_\mathrm{avg} = \frac{1}{2} P B_0 \omega. \tag{2.20}$$

Thus, Cox successfully derived the field force which depends on the dipole movement, frequency, and magnetic field. He suggested the use of water as a possible propellant due to its second highest dipole movement-to-mass ratio in permanently polarized fluids. Reference [9] provides Cox's conceptualization of such a propulsion engine. But at the time, he also expressed concerns about developing a technology for switching stationary coils at the high magnetic field energies and at very high frequencies required.

In 1985, Micci [12] demonstrated that it was not possible to achieve dipole propulsion at that time. The force obtained by using naturally occurring substances was too small and electronically excited atoms or molecules were found to be unstable. Sufficiently high strength/high frequency field generation technologies were not available. Thus, the concept of such an electromagnetic thruster working with the Abraham force using non-ionized dipole gases by Cox was not feasible in the 1990s.

2.2 Contemporary Developments

As shown above, dipole propulsion has been an open research subject since the 1980s. Cox showed the force acting on the dipole in varying electric and magnetic fields to be directly proportional to magnetic field strength, frequency, and dipole movement. In 2009, Paunescu did a thorough

Masters' thesis on the subject of dipole propulsion [13]. He did molecular dynamics simulations and experiments on the prospect of using the Abraham force for propulsion using a steady magnetic field instead of an alternating one. He explicitly compares the use of lithium hydride and water as propellants and their behavior in various electric and magnetic fields. Lithium hydride has the highest and water has the second highest naturally occurring dipole moments. Constant, square, saw-tooth, and sinusoidal electric profiles were simulated at different frequencies and pressures and the viable waveforms were tested experimentally.

Figure 2.2 shows the simulation results with a water molecule modelled as a two-particle dipole for ease of simulation. There is a sawtooth electric field with a strength of 20,000 V/m and a steady magnetic field of 25 T. Paunescu was also familiar with the effects of intermolecular collisions on such a molecular dynamics simulation. He studied the collision frequency and applied its effects on the single molecule he was simulating. For a sawtooth profile, the collisions were deemed useful when the electric field was off for equal distribution of energy and deemed unwanted when the molecules were accelerating under the effect of an electric pulse. Understanding this was crucial for the concept to work. The simulation resulted in an average acceleration of 5.5×10^5 m/s^2 [13].

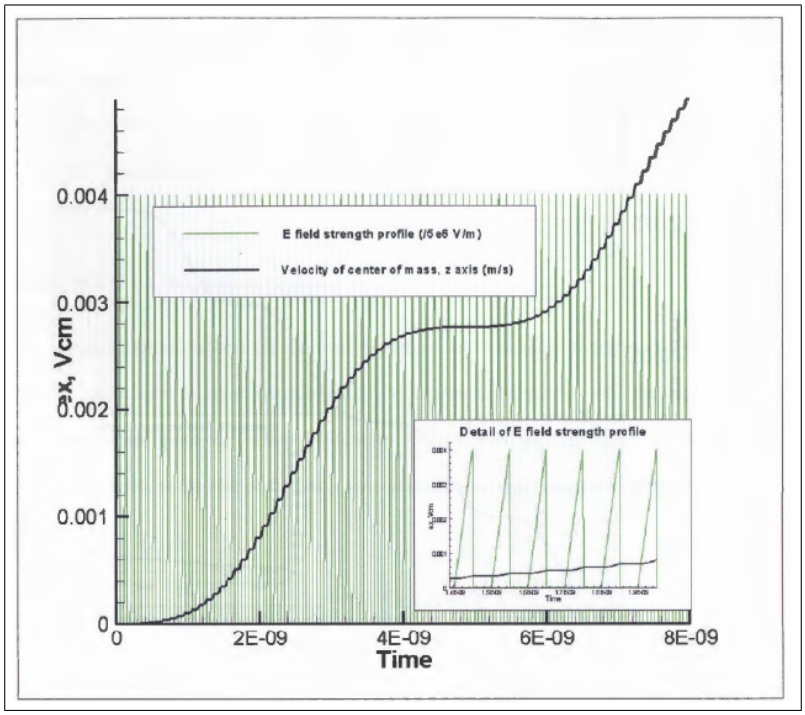

Figure 2.2. Molecule center of mass velocity in electric field strength sawtooth profile [13]

The results he obtained encouraged him to look into pulsed electric fields. With an electric field strength of 20,000 V/m and static magnetic field of 25 T, Paunescu studied the effects of frequency and duty cycle of pulsed electric field on acceleration. The maximum acceleration he obtained was 4.96×10^6 m/s^2 [13]. He then chose pressure and collision frequency as independent

variables for different types of electric field profiles in an attempt to find the optimum values.

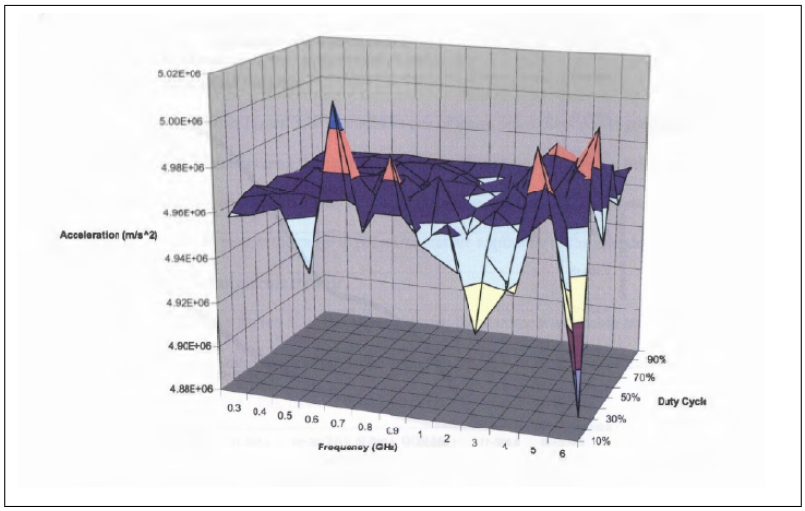

Figure 2.3. Acceleration from a pulsed electric field strength; effect of frequency and duty cycle [13]

To validate the simulation results obtained, he performed an experiment within a quartz tube. A non-static vinyl plastic curtain of surface resistivity of 10^6 ohms and 0.8 mil thickness called a 'flapper' was inserted in the center of the quartz tube to indicate any changes in the flow rate of the water vapor. He recorded results with a low DC voltage, a high DC voltage and a pulse generator. The experimental frequencies ranged from 100 Hz–250 MHz, a constant magnetic field generated by a permanent magnet of 0.6 T, and an electric field strength of approximately 88 V/m. Unfortunately, due to the time constraints, his experiment did not show any acceleration.

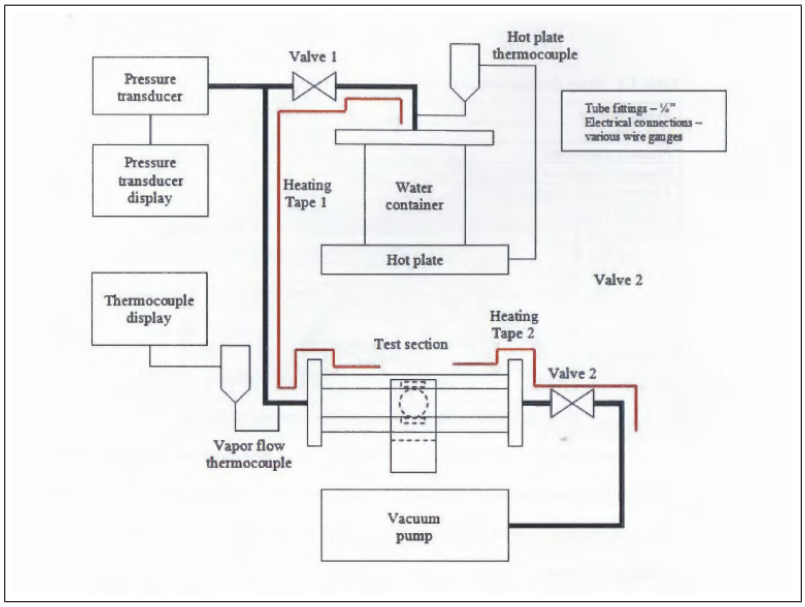

Figure 2.4. Experimental setup [13]

Paunescu's results did lay the foundation for future exploration of the dipole propulsion concept. Based on all the knowledge he obtained from the simulations and experiment, he suggested some parameters for future exploration. The parameters were a constant 25 T magnetic field, a sawtooth or sinusoidal electric field profile of any strength up to breakdown, and a frequency of 250 Hz–30 GHz. His simulations were the first to successfully demonstrate the acceleration of dipole molecules under a steady magnetic field and varying electric field both acting in perpendicular directions.

Contri [14] furthered Paunescu's research. He compared the three probable propellants lithum hydride, rydberg atoms, and water molecules based on their dipole strengths, stability, and availability. He demonstrated that the use of water is most beneficial for reasons including its abundance, availability, and status as a green propellant. Contri also compared the various initial orientations of the water molecule dipole for a maximum velocity increase. Using molecular dynamics simulations, he concluded that, if the water molecule lies in the x-z plane with the hydrogen atoms rotating along the x axis, a velocity increase of approximately 0.58 mm/s is achieved for a static magnetic field of 25 T and a single cycle sinusoidal electric field of 21 kV/m at 75 GHz [14]. He then extended his molecular dynamics simulations to 1000 water molecules. The conclusions of his thesis are used as the basis for this research.

The molecular dynamics simulation of 1000 water molecules was considered as the first step to study the bulk behavior of propellant in this research. Working with a multiple-molecule simulation proved better for understanding of intermolecular interactions on the acceleration process. A successful simulation with 1000 water molecules can be the closest replica for an actual working experiment so far. The goal of this research is to demonstrate the acceleration obtained from a multiple molecule simulation using a steady magnetic field and a varying electric field. That acceleration obtained can be then compared with current electric propulsion techniques using ionized propellant.

Chapter 3

Computer Simulations

Molecular dynamics, a type of computer simulation method, is used to study the motions of atoms or molecules interacting within a simulation environment. The paths of the atoms and molecules can be monitored by solving the equations of motion for a certain time period in which they are allowed to interact [15]. The applications of molecular dynamics simulations include chemical physics, material science, and modelling of biomolecules.

The method of molecular dynamics is used in this research to simulate the Abraham force conditions. The simulation environment has a sinusoidally varying electric field acting in the x direction and a steady magnetic field in the y direction. 1000 water molecules are given initial positions and velocities in the simulation volume. The simulation volume is a cube that has its length calculated by

$$l = \left(\frac{nk_{\mathrm{b}}T}{P}\right)^{\frac{1}{3}}, \tag{3.1}$$

where n is the number of molecules. The positions are defined keeping in mind the geometry of a water molecule. Initially, all the molecules have similar orientation. The two hydrogen and one oxygen atom have a bond length of 1 Å each and the bond angle between the two hydrogen atoms is 109.5°. The initial velocities are defined based on a Maxwellian distribution. The time span for the simulations is in picoseconds ranging up to 1000 ps. A lot of parameters like the electric field strength, frequency, pressure, and magnetic field strength had to be specified. Temperature for most of the simulations is assumed 500 K. The pressure and electric field strength had a limiting value for the propellant to be comprised of neutral water vapor molecules. Detailed explanation for this is given in Section 3.1. A steady magnetic field strength of 25 T is used as proposed by Paunescu in his thesis. Different values for frequency are tested including 50 GHz, 75 GHz, and 100 GHz. The force derived by Cox was directly proportional to frequency and thus microwave frequencies were used here.

Once all the working parameters were specified, understanding of the molecular dynamics simulation procedures was important. Molecular dynamics simulations use various algorithms

for updating the velocity and positions at every time step. Comparisons of various available algorithms and the ones used for this research is described in Section 3.2. Along with the constraint and Verlet algorithms, periodic boundary conditions are used to keep the molecules constrained in the simulation volume. If a molecule tries to escape the simulation volume from any side while accelerating, it is shifted back to the end of the opposite side in the exact same orientation and it continues its motion towards that side again.

The final goal of the simulations is to calculate the acceleration from multiple molecules, and compare it with current electric propulsion techniques. If the calculated acceleration falls in the range of current electric propulsion methods, it would mean that dipole propulsion has potential as a realizable propulsion method. It can be validated as a highly efficient electromagnetic propulsion system. But before calculating the acceleration produced by the simulations, it was important to demonstrate the stability of the system. Any control volume should demonstrate conservation of energy, momentum, and polarity. The total energy and momentum has to be conserved throughout the acceleration process of dipole propulsion. Thus, simulations for calculating and plotting the total kinetic energy and momentum are described in Sections 3.3 and 3.4.

3.1 Electric Field Strength

For the Abraham effect to work, the water vapor entering as propellant should contain neutral water vapor molecules versus ionized water vapor molecules. To avoid the ionization of water molecules, their breakdown characteristics need to be known. Breakdown can occur at low pressure or high electric field strength. Figure 3.1 shows a Paschen curve for a low pressure water vapor environment being exposed to microwave radiation. It is evident that there is a limit for pressure and electric field strength to avoid the breakdown of the water molecules. This is the result of a study by Bandel and MacDonald [16] and it is relevant to dipole propulsion because it outlines water-vapor environments with low DC voltage, high DC voltage and pulse-generated electric fields at microwave frequencies. The pressure range for their experiment was 5 to 50 Torr and the electric field strength was in the range of 0 to about 1200 V/cm. It only reached close to the breakdown strength at 1176 V/cm during the high DC voltage test. That implies a maximum limit of 117.6 kV/m to keep the propellant entering the system of dipole propulsion neutral. According to Contri's research, the optimum value of electric field strength of 21 kV/m falls within this acceptable range. A pressure of 3000 Pa, which is approximately 22.5 Torr, is used for the simulations here and field strengths of 50 kV/m and 100 kV/m are explored.

3.2 Molecular Dynamics Algorithms

Molecular dynamics is used here to simulate the Abraham force environment. The molecular behavior and the intermolecular interactions are monitored by using molecular dynamics al-

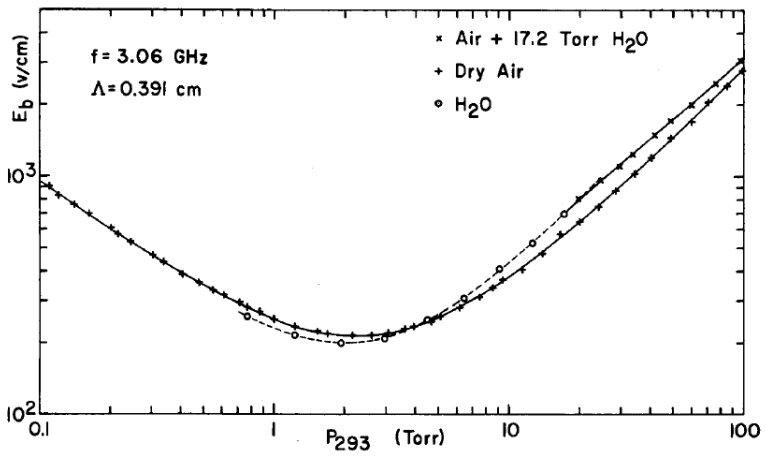

Figure 3.1. Breakdown rms field strength versus total pressure with 100-μsec pulse length [13]

gorithms. A constraint algorithm is used to constrain the bond lengths of the atoms in the molecules. After defining the initial molecule positions and velocities, the constraint algorithms are used. It alerts about a constraint failure whenever the distances between either two hydrogen atoms or between hydrogen and oxygen atoms deviate from the accepted values.

The velocities are updated by RATTLE, an algorithm for integrating the equations of motion for molecules subject to intramolecular constraints [21]. After calculating the forces, the 'first velocity Verlet' advances the position by a full time step and the velocity by half a time step as follows:

$$\begin{aligned} \vec{r}(t+\Delta t) &= \vec{r} + \Delta t\vec{v}(t) + \tfrac{\Delta t^2}{2}\vec{a}(t) \text{ and} \\ \vec{v}(t+\tfrac{\Delta t}{2}) &= \vec{v}(t) + \tfrac{\Delta t}{2}\vec{a}(t). \end{aligned} \tag{3.2}$$

The forces are then updated again and the 'second velocity Verlet' advances the velocity by other half time step:

$$\vec{v}(t+\Delta t) = \vec{v}\left(t+\frac{\Delta t}{2}\right) + \frac{\Delta t}{2} + \frac{\Delta t}{2}\vec{a}(t+\Delta t). \tag{3.3}$$

The acceleration appearing in the equations is simply calculated by dividing the total calculated force by the mass. The RATTLE algorithm determines the positions and velocities at the current time step to order t^2 with a minimized round-off error [21].

3.2.1 Constraint Dynamics

A constraint algorithm is a method for satisfying the Newtonian motion of a rigid body consisting of points of mass by ensuring that the distances between the points of mass are maintained. The relations of the constraint remain perfectly fulfilled at each step of the trajectory despite the approximate character of numerical integration [22]. In the presented molecular dynamics simulations, movement of the molecules in all the degrees of freedom is not desirable. For example monitoring the vibration of the atoms of the water molecule would be a waste of the simulation

space and time. The constraint algorithm verifies the fixed bond lengths for the water molecule each time its position is updated. By monitoring the lengths between the H–H and two O–H bonds, the bond angle between the hydrogen atoms is already taken care of. In the absence of any constraint algorithm, the bond lengths or the bond angles between the atoms of the molecule can get distorted resulting in errors or extended simulation times.

SHAKE and RATTLE are two of the many widely used molecular dynamics algorithms. The Lagrange multiplier–based methods like SHAKE or RATTLE retain the simplicity of Cartesian coordinates and avoid many of the complications of Euler angles and quaternions while incorporating the effects of the constrained geometry of the molecule [21]. But an important drawback of the SHAKE algorithm is that the velocity is not one of the variables used for integrating the equations of motion. Thus, Anderson suggested a velocity variant of the SHAKE algorithm called the RATTLE algorithm. The RATTLE algorithm functions similar to SHAKE, but has velocity as one of its variables as well. If we know the positions, velocities, and forces at one time step, we can calculate the positions at the next time step using Equation 3.1, which satisfies the constraint algorithm. Then, when we have the positions at the next time step, we can calculate the forces and integrate them using the RATTLE algorithm to calculate the velocities. This is exactly how the molecular dynamics simulations presented here proceed from one time step to another. It starts with the initially defined positions and velocities, calculates the molecular forces, and the first velocity Verlet updates the position by a complete time step following the constraints. Then the molecular forces are calculated again for the updated positions and those are integrated by the second velocity Verlet for velocities at the next time step.

3.3 Molecular Forces

Three types of forces acting on the molecules are taken into consideration for the molecular dynamics simulations:

1. Lorentz Force
2. Coulomb's Force
3. Lennard-Jones Force

The simulations are carried out for a 1000 ps time span. A single cycle sinusoidal x direction electric field pulse of 21 kV/m is applied at 520 ps. A static magnetic field of 25 T acts in the y direction. The forces calculated are integrated to find the velocities, which are used for calculating the kinetic energy. The total kinetic energy is calculated for 1000 molecules and then is averaged. Explanation of each forces and their calculation methods follow.

Lorentz force exists when there is an electric field and a magnetic field due to electromagnetic interaction. When a charged particle with charge q is moving with a velocity v, in the presence of magnetic and electric fields, the Lorentz force acting on it is given by

$$\vec{F}_{\mathrm{L}} = q(\vec{E} + \vec{v} \times \vec{B}) \tag{3.4}$$

The same equation is used in the molecular dynamics simulation here to calculate the Lorentz Force in the *x, y*, and *z* directions based on the velocity, electric field strength, and magnetic field strength in the *x, y*, and *z* directions, respectively.

The Coulomb force is the result of interaction between two charged particles. The force is calculated between the charges of a dipole and among the molecules. According to the Coulomb's relation, i.e.,

$$\vec{F}_{\mathrm{C}} \propto \frac{q_1 q_2}{r^2}, \tag{3.5}$$

the force is inversely proportional to the square of the distance between the particles. Therefore, the force decreases as the distance between the charges increases. In the past, the Ewald method, which used that Fourier series, was the most employed computational method in molecular dynamics simulations for calculating the Coulomb force. Solution of the Fourier series required a lot of computational time. In 1999, Wolf presented a method for calculating the Coulomb force revolving around the concept that the force keeps decreasing as the distance between the particles increase. Wolf's method reduced the computational time from that of Ewald method by a factor of 2 to 3 because it did not use the Fourier series [18]. Wolf gave a formula for directly calculating the Coulomb force. The formula has a cut-off radius r_{c}; if the distance between the charges is more than this cut-off radius, then the force becomes negligible and is considered to be zero. For distances less than the cut-off radius, the Coulomb force is given by

$$\vec{F}_{\mathrm{C}} = q_1 q_2 \left(\frac{\mathrm{erfc}(\alpha r)}{r^3} - \frac{\mathrm{erfc}(\alpha r_{\mathrm{c}})}{r_c^3} \right) \vec{r} + \frac{2\alpha}{\sqrt{\pi}} \left(\frac{\exp(-\alpha^2 r^2)}{r^3} - \frac{\exp(-\alpha^2 r_{\mathrm{c}}^2)}{r_{\mathrm{c}}^3} \right) \vec{r}, \tag{3.6}$$

where

$$\mathrm{erfc}(\alpha r) = 1 - \frac{\alpha r}{r_{\mathrm{c}}}. \tag{3.7}$$

The best-suited values for the parameters α and r_{c} for water molecules are selected from George's paper [19].

The interaction between the molecules was also affected by the Lennard-Jones potential. The simple truncation method [20] is used for the calculation of Lennard-Jones force. The method has a cut-off radius similar to the Coulomb force calculation. This method gives fairly accurate results because the Lennard-Jones force is a short range interaction and becomes negligible as the distance between the particles increases to beyond the cut-off radius. The force is given by

$$\vec{F}_{\mathrm{LJ}} = 24\epsilon \left(\frac{2\sigma^{12}}{r^{14}} - \frac{\sigma^6}{r^8} \right) \vec{r} \tag{3.8}$$

for distances smaller than r_{c} and zero everywhere else. r_{c} is usually 2.5σ. The Lennard-Jones parameters σ and ϵ for water are shown in Table 3.1 [20].

All the three forces are then added together in respective directions and integrated using the velocity Verlets. The velocities calculated by the velocity Verlet are then used in the calculation of the total kinetic energy, i.e.,

$$\mathrm{KE} = \frac{mv^2}{2}. \tag{3.9}$$

Table 3.1. L-J parameters for all L-J interactions between two water molecules.

Atomic Interaction	σ [$\AA$]	ϵ [J]
H-H	2.81	$8.6k_{\mathrm{b}}$
O-O	2.95	$61.6k_{\mathrm{b}}$
H-O	2.88	$23.0165k_{\mathrm{b}}$

The simulations run for a 1000-ps time span, i.e., 10,00,000 time steps. Energy is re-scaled up to half of the time steps which is 500 ps by using a re-scaling factor f given by

$$f = \sqrt{\frac{\mathrm{KE_{ave,i}}}{\mathrm{KE_{ave}}}} \tag{3.10}$$

where $\mathrm{KE_{ave,i}}$ is the initial average kinetic energy and $\mathrm{KE_{ave}}$ is the average kinetic energy at every 1000^{th} time step. The re-scaling helps to bring back the energy to the initial value for half of the time steps. The total average kinetic energy then remains constant when the re-scaling is removed after 500 ps time span. Thus, energy in the system is conserved.

3.4 Momentum

Conservation of momentum is also essential to monitor. Momentum is simply the product of mass and velocity. For calculating the momentum in these molecular dynamics simulations, the mass-weighted average of the directional velocities is calculated. The *x, y*, and *z* velocities for oxygen are multiplied by 16 and for hydrogen by 1 and are added together. The average velocities are then divided by the mass of molecule, which is 18, and the number of molecules. Mass-weighted average momentum is then calculated by taking the square root of the squares of directional velocities added together, i.e.,

$$p = \sqrt{v_x^2 + v_y^2 + v_z^2}. \tag{3.11}$$

Simulation time is 1000 ps again with a single sinusoidal electric field pulse of strength 21 kV/m acting at 520 ps.

The *x, y*, and *z* velocities are re-scaled up to half of the time steps by subtracting the mass-weighted average velocities from the calculated velocities. The mass-weighted average momentum with the velocity re-scaling is then plotted. The plot shows the conservation of momentum and, when the re-scaling is removed after 500 ps, momentum is still conserved.

3.5 Polarities

The importance of plotting the total polarity and polarities in the *x, y*, and *z* directions is to monitor the conservation of total polarity and see the effect of the electric pulse on the molecule

orientations. The simulation was run for a 1000 ps and a single sinusoidal electric field pulse was applied at 520 ps as used for all the other simulations.

To plot the polarities accurately, the simulation was scaled down to one molecule. Initial polarity was dependent on the initial orientation of the molecule. There can be many ways for defining the initial position of a single molecule. Working from the results obtained by Contri for maximum acceleration of a single molecule, the x-y plane and the x-z plane orientations were the probable options. For monitoring the polarity conservation here, the initial position was defined for a single molecule in the x-y plane in such a way that the resultant polarity was only non-zero in the y direction. The oxygen atom was at the origin, one hydrogen in the first quadrant and another in the second quadrant with an angle of 109.5° between them. Polarity is calculated by the formula:

$$P_x = q_1(H1_x + H2_x) + 2q_2(O_x), \tag{3.12}$$

$$P_y = q_1(H1_y + H2_y) + 2q_2(O_y), \text{and} \tag{3.13}$$

$$P_z = q_1(H1_z + H2_z) + 2q_2(O_z), \tag{3.14}$$

where q_1 is 6.79 $\times 10^{-20}$ C, the charge on a hydrogen atom and q_2 is -1.358×10^{-19} C, the charge on an oxygen atom. $H1$, $H2$ and O are the position vectors for hydrogen 1, hydrogen 2, and oxygen, respectively. The total polarity is given by

$$P = \sqrt{P_x^2 + P_y^2 + P_z^2}. \tag{3.15}$$

Theoretically, the total polarity remains constant and the individual polarities respond to the applied electric field pulse to indicate its effect on the molecule orientation. The molecular dynamics simulations results actually show that the molecule initially was orientated from the x-y plane to the x-z plane. Maximum y polarity reduced to near zero and the zero z polarity became maximum conserving the total polarity. The oxygen atom revolved around the x axis and the hydrogen atoms moved from the x-y plane to the x-z plane. This occurred in less than 50 ps. The orientation then remained constant in absence of any interactions, but responded to the electric pulse at 520 ps as a momentary increase in the x polarity.

Animation of a single molecule was created to verify the plot. The animation showed the molecule rotating from the x-y plane orientation to the x-z plane orientation in the initial 50 ps and then tilt just a little towards the x plane and back during the application of the electric pulse.

Initial velocity was then changed to see the effect on the initial rotation of the molecule. Five random initial velocities with different directions were picked and the plots were generated with a single sinusoidal electric pulse applied of strength 21 kV/m. The direction of the velocity did affect the initial rotation of the molecule, but the maximum velocity increase was achieved with the randomly generated Maxwellian velocities used originally.

The next challenge was to graph the polarities of 1000 molecules. This was a relatively difficult task as the intermolecular interactions came into the picture. The better way to achieve

that was to increase the number of molecules gradually, i.e., plot for 1, 5, 10, 100, and then 1000 molecules. When using a lower number but more than one molecule, it was essential to find the appropriate separation distance. Otherwise the distance between the molecules fell in the negligible range rendering it impossible to calculate the forces between them. Chapter 4 shows the polarity plots and acceleration calculation for a single and multiple molecules simulations. Acceleration was calculated at various frequencies, electric field strengths, initial orientations, and initial velocities.

Chapter 4

Results

The final goal of the research was to calculate the acceleration for dipole propulsion from molecular dynamics simulations and compare it with the current electric propulsion techniques using ionized gases. This chapter shows the acceleration calculated from a single molecule and multiple molecules using molecular dynamics simulations. The concept of simulating the Abraham force by a varying electric field in the x direction and a steady magnetic field in the y direction promised an acceleration of the propellant molecules in the z direction. The simulations showed a continuous increase in velocity in the z direction. The acceleration is thus calculated by recording the z velocity at the exact time step, once with the electric pulse and once without the electric pulse and using the formula:

$$a = \frac{v_2 - v_1}{tn}, \tag{4.1}$$

where t is the time period which is the inverse of the frequency used and n is the number of pulses applied. Single-pulse simulations are done up to 60 ps with the electric field pulse acting at 35 ps. For multiple pulse cycle simulations, the time period is increased to accumulate all the pulses. The individual parameters used for each simulation is listed in the respective sections.

4.1 Single Molecule

The polarity and acceleration calculations were first scaled down to single molecule. If the molecular dynamics simulation for a single molecule works as desired and gives the desired acceleration, the same procedure can be then used for accelerating multiple molecules. All the results shown in this section for a single molecule were obtained under the same conditions for the purpose of comparison. The conditions are as listed in Table 4.1. The simulation cube volume is calculated at 3000 Pa pressure and 500 K temperature using

$$V = \frac{nk_{\mathrm{b}}T}{P}. \tag{4.2}$$

Table 4.1. Conditions used for generating single molecule plots.

Quantity	Value	Direction
Number of molecules	1	
Electric field	50 kV/m or 100 kV/m	x
Magnetic field	25 T	y
Pressure	3000 Pa	
Temperature	500 K	

For the initial orientation of the molecule, both the x-y plane orientation and the x-z plane orientation as shown in Figure 4.1 were tested. Results showed that both the orientations gave the same acceleration. All the results presented here have the initial x-y plane orientation in which the molecule lies in the x-y plane such that the y polarity is maximum and x and z polarities are 0. Electric field strengths of 50,000 V/m and 100,000 V/m (both below breakdown of 117.6 kV/m) were tested to examine their effects on the acceleration. A constant y-direction magnetic field of 25 T remained unchanged. The final acceleration plot was generated at three different frequencies: 50 GHz, 75 GHz, and 100 GHz. The initial velocity assigned in each direction is listed on the respective plots.

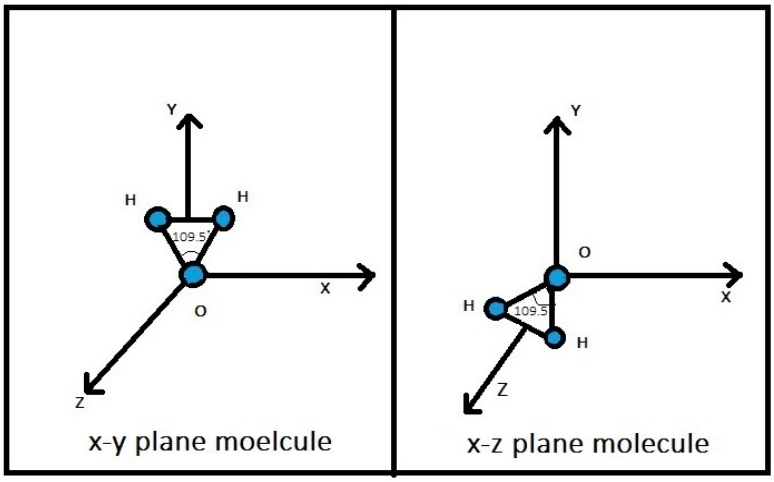

Figure 4.1. x-y and x-z initial orientations of water molecule (not to scale)

Before jumping to a moving molecule simulation, the effect of the perpendicular electric and magnetic fields was first studied on a stationary water molecule. A stationary molecule should not show any movement in just the y-direction constant magnetic field, but should show some velocity increase on application of the sinusoidal electric field pulse to validate the Abraham effect. Figure 4.2 shows the x, y, z values, and the total polarity with the electric pulse of 50

kV/m at 75 GHz frequency while Figure 4.3 shows the velocity in the z direction with the electric pulse.

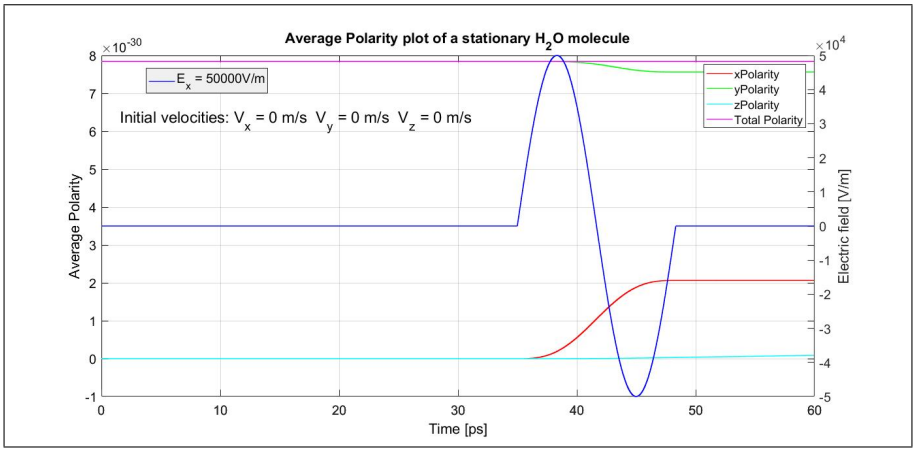

Figure 4.2. Polarities of a stationary molecule under perpendicular electric and magnetic fields

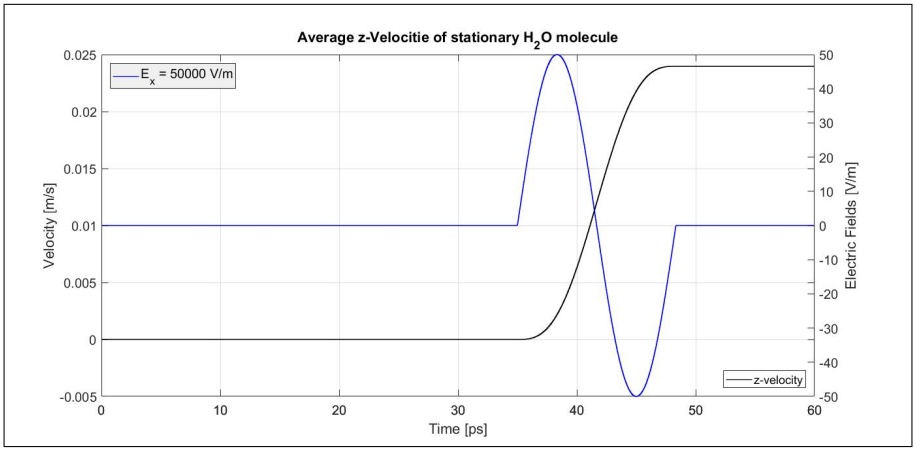

Figure 4.3. z-direction velocity of a stationary molecule under perpendicular electric and magnetic fields

Both results clearly showed that there is no movement of the stationary molecule in the magnetic field. Only when the perpendicular electric field is applied, does the molecule change its orientation under the effect of the electric pulse, as well as show a velocity increase in the z-direction on application of electric pulse. The acceleration obtained in these results formed the basis to demonstrate the Abraham effect.

The next aim was to see the effect on a thermally moving molecule. Taking one step at a time, individual directional velocities were applied with no electric pulse. With an x velocity of 100 m/s, the molecule showed movement under the y direction magnetic field as seen in Figure 4.4. The molecule tries to orient from the x-y plane to the x-z plane. The x polarity remains constant under no electric pulse. The molecule rotates about the x axis in a manner that the hydrogen atoms move to the x-z plane with maximum positive z polarity.

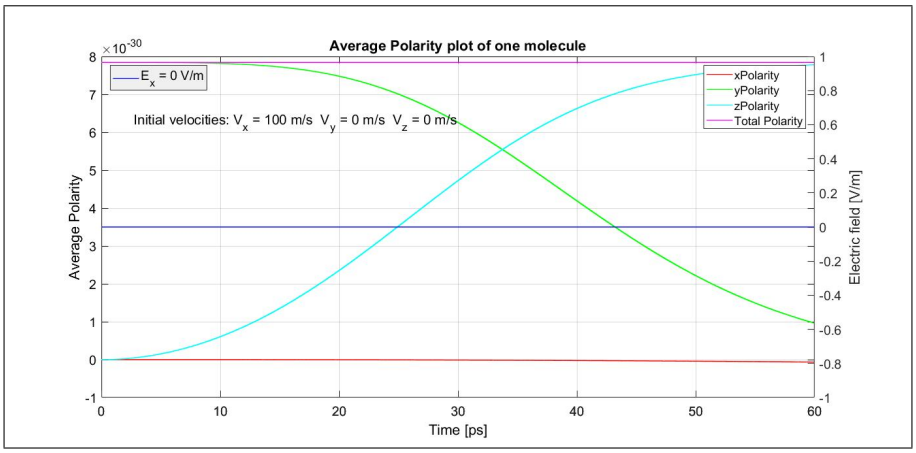

Figure 4.4. Polarity of a molecule only moving in the x-direction

Now keeping the velocity in the x and z directions to be 0 m/s, the velocity in the y-direction was changed to 100 m/s. The molecule here is moving in the direction of the magnetic field and, thus, no change is seen in Figure 4.5 in the orientation of the molecule. The molecule does not rotate at all.

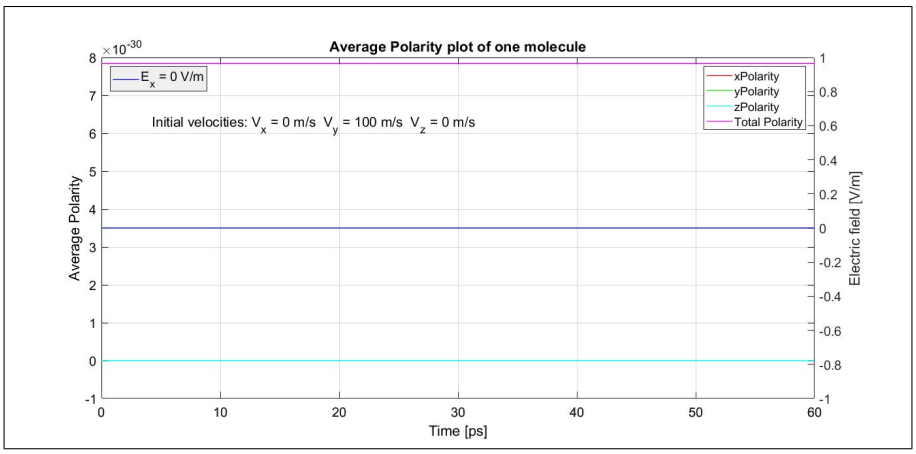

Figure 4.5. Polarity of a molecule only moving in the y-direction

Finally, the molecule is given only a z-directional initial velocity of 100 m/s. As shown in Figure 4.6, the polarities change in yet another fashion. The molecule stays in the x-y plane in which it is defined but it starts rotating about the z axis. Thus the z polarity is not affected but both the y polarity reduces and the x polarity goes in the negative direction.

Moving one step further, the molecule was given an initial velocity of 100 m/s in each direction, which made the net velocity of approximately 173.2 m/s, equivalent to a translational temperature of approximately 390 K calculated by

$$v = \left(\frac{3RT}{M}\right)^{0.5}. \tag{4.3}$$

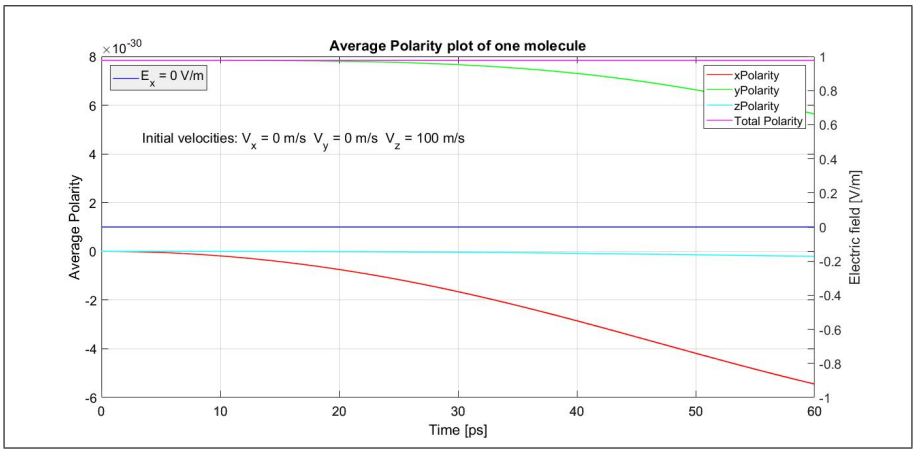

Figure 4.6. Polarity of a molecule only moving in the z-direction

A single electric pulse of 50,000 V/m was applied at 75 GHz frequency. As seen previously, the molecule first oriented in the x-z plane. The x polarity also changed due to the velocity of the molecule in all three directions. The effect of the pulse was clearly visible as a momentary change in the orientation as shown in Figure 4.7. The calculated acceleration during the pulse was 1.797×10^9 m/s^2.

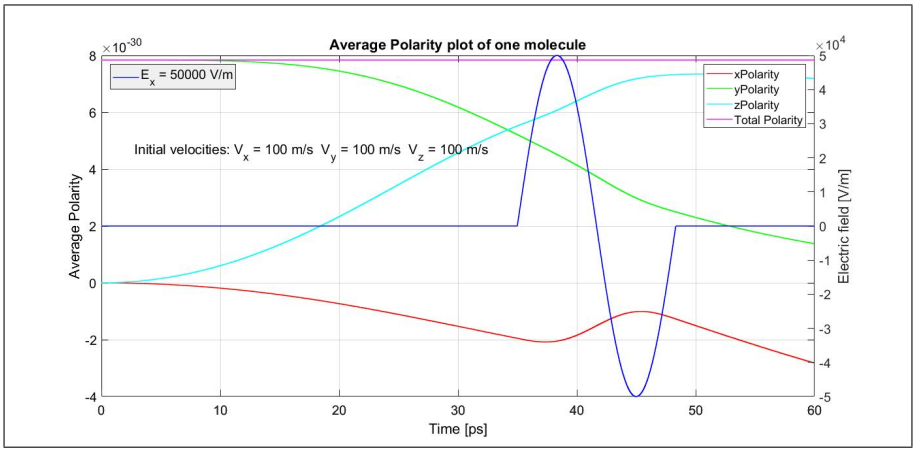

Figure 4.7. Polarity of a thermally moving molecule

The current electric propulsion techniques have an acceleration in the range of 10^{11} m/s^2. To close that gap with dipole propulsion, the first step was to increase the number of pulses and study the effect on the acceleration. The number of pulses were increased and the acceleration corresponding to each was tabulated. To show a few results, the polarities with 5 and 50 electric pulse cycles are plotted in Figures 4.8 and 4.9, respectively, with the electric field strength of 50,000 V/m. Figure 4.8 shows changes in all the three directional polarities with the application of the electric pulses. The molecule changes orientation in the same fashion each time an electric pulse is applied, still conserving the total polarity. Similar changes are seen in Figure 4.9 with 50

electric pulses. Every time an electric pulse is applied, the molecule orients in the exact similar manner. The changes in the orientation stop as soon as the electric field goes to 0 V/m.

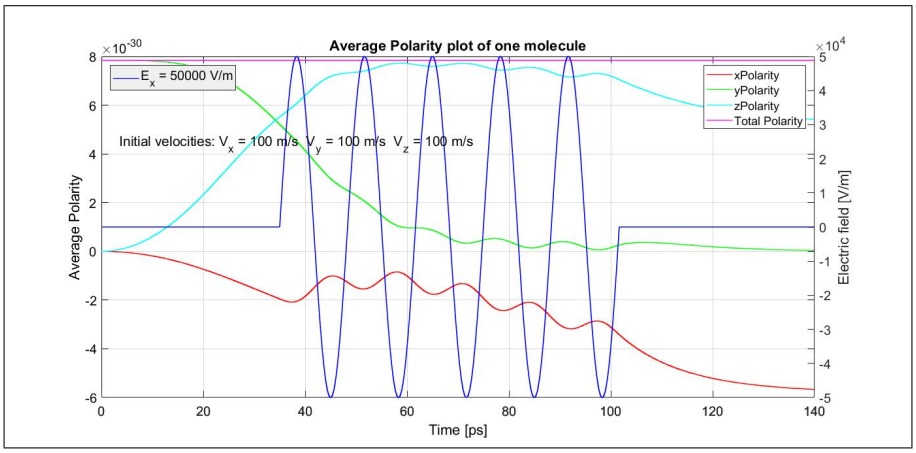

Figure 4.8. Polarity of a molecule with five cycles applied

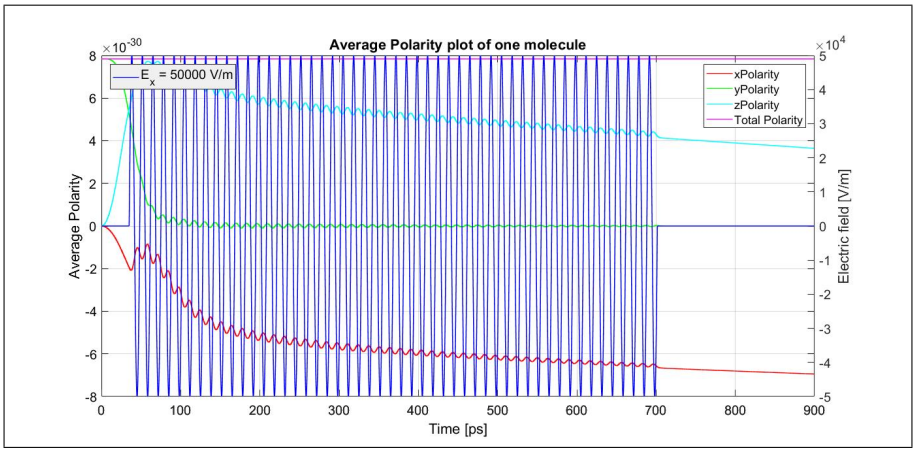

Figure 4.9. Polarity of a molecule with fifty cycles applied

It was also essential to test the range of frequencies and electric field strengths. The goal here is to find the maximum acceleration at optimum conditions. 50 kV/m and 100 kV/m electric field strengths were tested at 50 GHz, 75 GHz, and 100 GHz. In Figure 4.10, acceleration changing with the pulse number is plotted for an electric field strength of 50,000 V/m at three different frequencies: 50 GHz, 75 GHz, and 100 GHz. For each frequency, the acceleration decreases with an increase in the pulse number. The acceleration was calculated up to the point where further increase in the pulse number leads to a 30% or more drop in the acceleration. Higher acceleration is achieved at lower frequencies. The maximum acceleration at 50000 V/m electric field is 2.696×10^{9} m/s^2 at 50 GHz.

The electric field strength is then increased to 100,000 V/m. Figure 4.11 shows the plot with 100,000 V/m electric field strength and frequencies of 50 GHz and 100 GHz. Once the

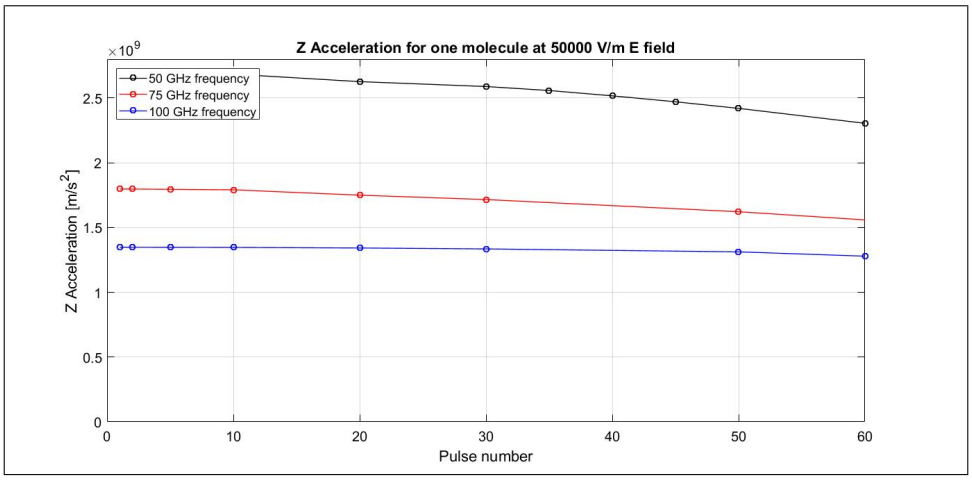

Figure 4.10. Acceleration dependent on the pulse number at 50,000 V/m

relation between the frequency and the acceleration was established, only the upper and the lower limits were plotted. The acceleration still decreases with increasing number of pulses as well as frequency. Maximum acceleration achieved is 5.393×10^9 m/s^2 for 100,000 V/m electric field strength and 50 GHz frequency. This acceleration is greater than the maximum acceleration obtained at 50,000 V/m. Table 4.2 shows the maximum acceleration corresponding to the pulse

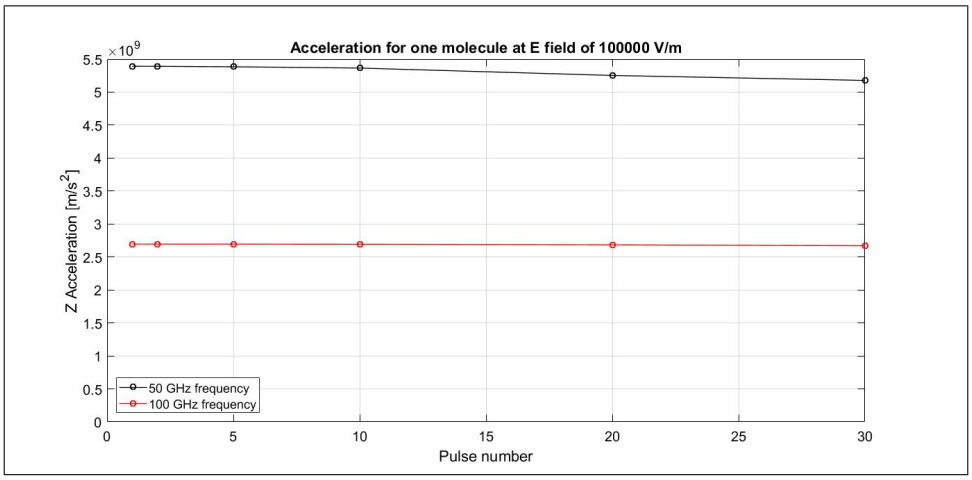

Figure 4.11. Acceleration dependent on the pulse number at 100,000 V/m

number, electric field strengths, and frequencies. For a single molecule the maximum acceleration that was achieved was 5.393×10^9 m/s^2 with 100,000 V/m electric field strength at 50 GHz. Single molecule simulations also showed that the acceleration increases with increasing the electric field strength and decreases with increasing the frequency.

Table 4.2. Acceleration comparison from plots for a single molecule

Acceleration [m/s^2]	**Pulse number**	**Electric field** [V/m]	**Frequency** [**GHz**]
5.393×10^9	1	100,000	50
2.696×10^9	1	50,000	50
2.696×10^9	1	100,000	100
1.797×10^9	1	50,000	75
1.348×10^9	1	50,000	100

4.2 Five Molecules

The polarity and acceleration simulations were then extended to five molecules. The conditions used for 5 molecules are shown in Table 4.3. The molecular separation distance was chosen

Table 4.3. Conditions used for generating 5 molecules simulations.

Quantity	**Value**	**Direction**
Number of molecules	5	
Electric field	50 kV/m or 100 kV/m	x
Magnetic field	25 T	y
Pressure	4000 Pa	
Temperature	300 K	
Molecular separation	1.73×10^{-1} m	

to be 1.73×10^{-1} m. For distances smaller than this, there were too many collisions of the molecules making it difficult to calculate the molecular forces, and distances higher than this had no significant effect on the orientation of the molecules. Cut-off radius for Coulomb force is 7×10^{-9} m and for lennard-Jones force is in the order of 10^{-10} m as shown in Table 3.1. Thus the 5 molecules should behave like a single molecule in absence of any intermolecular interactions. Figure 4.12 is the polarity plot obtained for 5 molecules with a x-direction single electric field pulse of 50,000 V/m at frequency of 75 GHz and y-direction magnetic field of 25 T. The initial velocities of all the molecules was defined to be 100 m/s in x, y, and z directions at 300 K temperature and 4000 Pa pressure. The plot obtained showed exact similar behavior to a single molecule.

To simulate for the maximum acceleration, an analysis similar to the single molecule was performed. Acceleration recorded at 50,000 V/m and 100,000 V/m electric field strengths at different frequencies are plotted in Figures 4.13 and 4.14, respectively. While the rate might differ, the acceleration still decreased with the increasing cycles similar to a single molecule. Maximum acceleration for each run was obtained with a single pulse. Increasing the frequency again lead to an decrease in the acceleration, while increasing the electric field strength lead to an increase in the acceleration. Maximum acceleration of 5.393×10^9 m/s^2 for 5 molecules was achieved at 100,000 V/m electric field strength and 50 GHz, very similar to a single molecule.

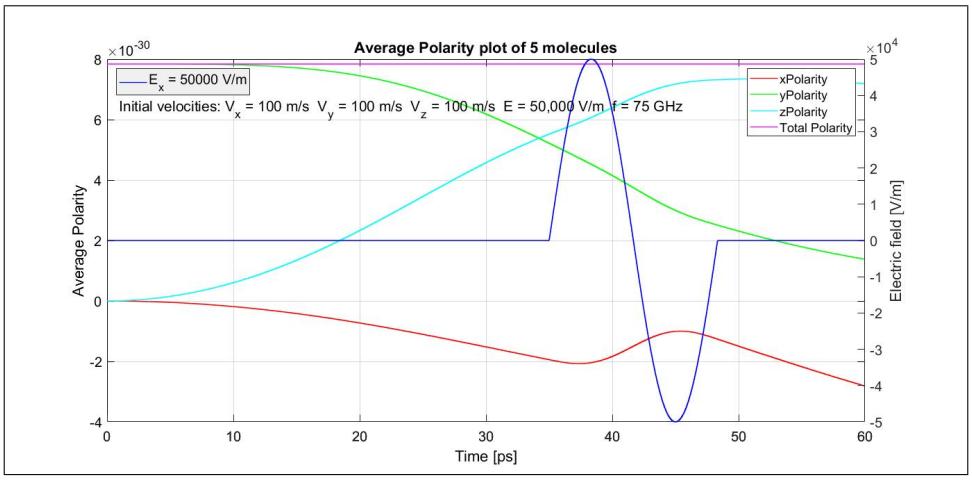

Figure 4.12. Polarity plot of 5 molecules

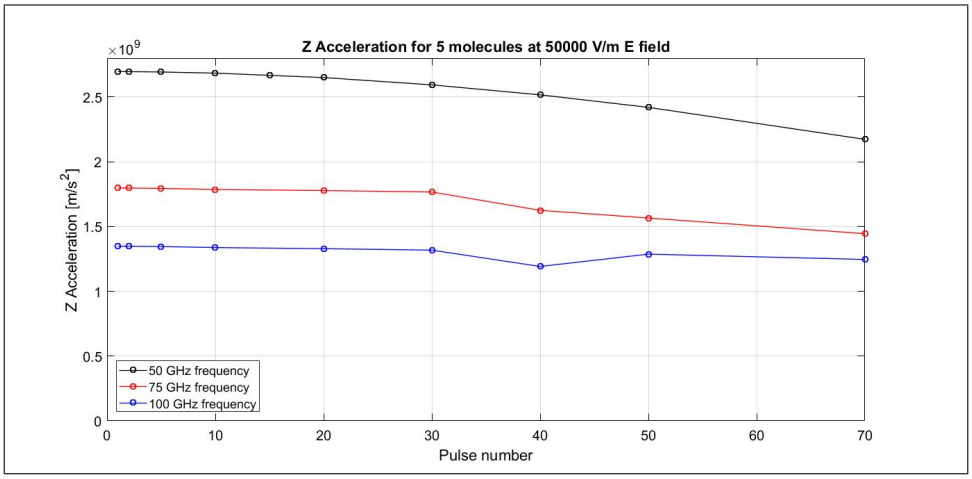

Figure 4.13. Acceleration dependent on the pulse number at 50,000 V/m

Tabulating the results of maximum acceleration for each run, the values are similar to a single molecule. The maximum acceleration obtained did not change.

For all the plots obtained above, the initial velocity was the same for all the molecules. This is not the real-life case. Thus, it was important to see the effect of random initial velocities for all water molecules. Here, the initial velocity is changed to a randomly generated Maxwellian distribution. The velocities are different for each molecule in each direction. The molecular separation distance was changed to 1.73×10^{-3} m. Acceleration was calculated as mentioned before and plots for acceleration versus pulse number were generated. Figure 4.15 shows the plot for 50,000 V/m electric field strength at frequencies of 50 GHz, 75 GHz, and 100 GHz. The relationship between the pulse number and acceleration was altered compared to previous plots. The values of acceleration remained similar initially at a low number of cycles for all frequencies, but as the pulse cycles increased, it lead to an increase in the acceleration. For all frequencies, the acceleration increased after 30 electric pulses. From Figure 4.15, it is visible that

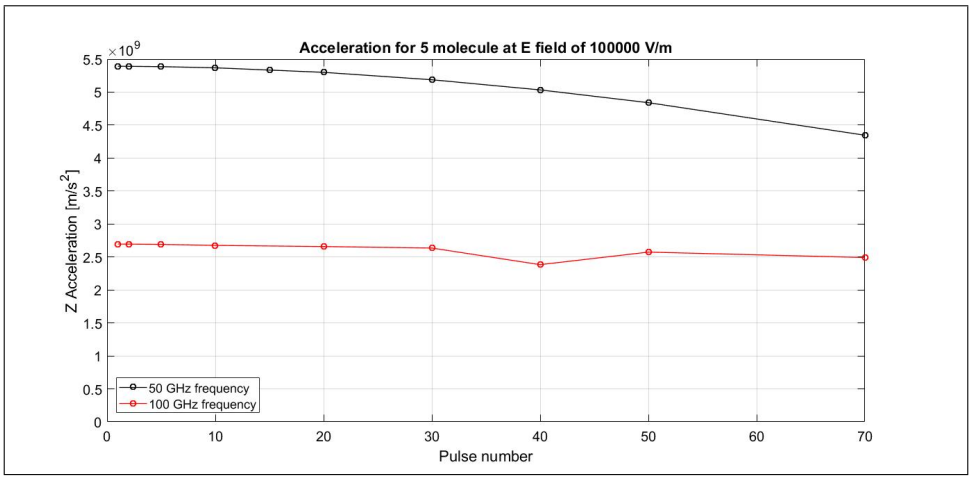

Figure 4.14. Acceleration dependent on the pulse number at 100,000 V/m

the maximum acceleration of 8.679×10^{11} m/s^2 was obtained at 75 GHz when 47 electric pulse cycles were applied. The highest acceleration increased from 50 GHz to 75 GHz, and decreased from 75 GHz to 100 GHz. Also for 50 GHz and 75 GHz, acceleration changed to deceleration when the electric field went over 50 cycles, and for 100 GHz it changed after 60 cycles. As 75 GHz gave the maximum acceleration, it encouraged to look into all the three frequencies at 100,000 V/m electric field strength. Figure 4.16 shows the acceleration-versus-pulse-number plot for 100,000 V/m electric field strength. Again, the 75GHz frequency gave the most acceleration of 1.011×10^{12} m/s^2 at 50 electric pulses. The acceleration peaked at 50 cycles for 50 GHz and 75 GHz, after which it became deceleration, whereas for 100 GHz, the acceleration peaked at 90 electric pulses. Comparing the maximum acceleration, it again showed increase from 50 GHz to 75 GHz and decrease from 75 GHz to 100 GHz. At 100 GHz, the acceleration peaked twice before turning into deceleration. Table 4.3 shows the results of maximum acceleration from Figures 4.15 and 4.16.

Table 4.4. Acceleration comparison from plots for five molecules

Acceleration [m/s^2]	**Pulse number**	**Electric field** [V/m]	**Frequency** [**GHz**]
1.011×10^{12}	50	100,000	75
6.35×10^{11}	90	100,000	100
8.679×10^{11}	47	50,000	75
4.427×10^{11}	50	100,000	50
4.284×10^{11}	50	50,000	100
2.604×10^{11}	43	50,000	50

From Table 4.3, it is clear that acceleration increased in 2 to 3 orders of magnitude with random Maxwellain distribution as initial velocities. This implies that the random velocities lead to more collisions of the molecules when there was no pulse and thus better orientation and better acceleration when higher number of pulses was applied. The optimum pulse number came

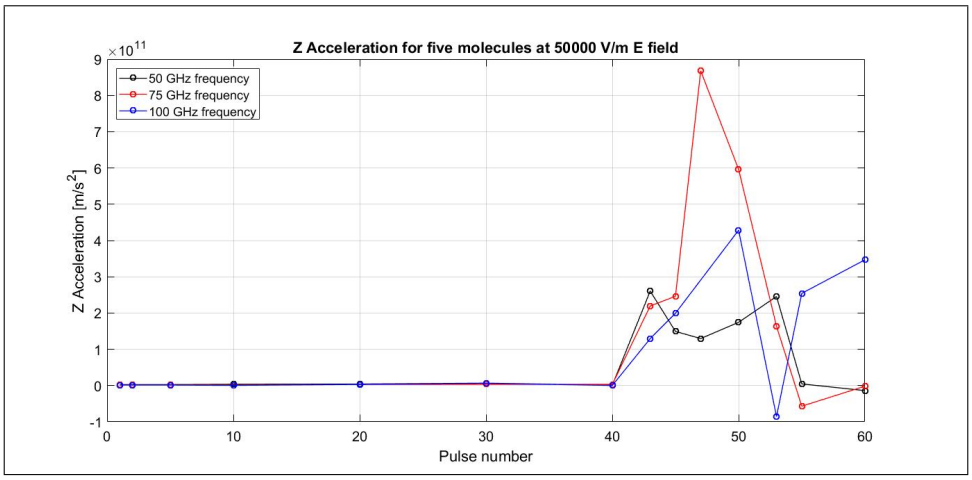

Figure 4.15. Acceleration dependent on the number of pulses with random initial velocities at 50,000 V/m

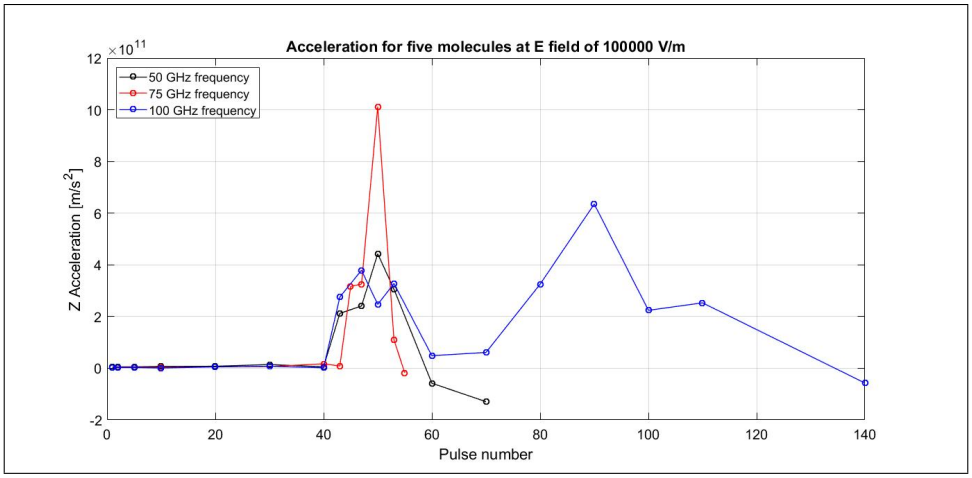

Figure 4.16. Acceleration dependent on the number of pulses with random initial velocities at 100,000 V/m

out to be 40 to 60 electric pulses at a frequency of 75 GHz. Electric field strength of 100,000 V/m gave better acceleration as the force is directly proportional to the electric field strength. As opposed to a single molecule, 5 molecules with the pulse cycle of 50 and frequency of 75 GHz gave the highest acceleration of 1.011×10^{12} m/s^2.

4.3 10 Molecules

The simulations were then extended to 10 water molecules. Again, all simulations were carried out at similar conditions for comparison purposes. The conditions are listed in Table 4.5. The purpose here is to show the acceleration of multiple molecules and also see the effect of number of electric field pulses, electric field strength and frequency on acceleration. The initial separation

distance between the ten molecules is 2.179×10^{-4} m, which was the smallest possible distance for calculating the molecular forces.

Table 4.5. Conditions used for generating 10 molecules simulations.

Quantity	Value	Direction
Number of molecules	10	
Electric field	50 kV/m or 100 kV/m	x
Magnetic field	25 T	y
Pressure	4000 Pa	
Temperature	300 K	
Molecular separation	2.179×10^{-4} m	

Simulation of a single and 5 molecules has showed so far that acceleration of water using the Abraham effect is possible. For 5 water molecules, the random Maxwellian distribution of initial velocities gave a higher acceleration value of 1.011×10^{12} m/s^2. Also the effect of pulse number and frequency on the acceleration produced varied. For 10 molecules, acceleration was calculated by two types of initial velocities. First was 100 m/s for each molecule in each direction, and second was randomly generated Maxwellian velocities, which gave a different velocity value for each molecule in each direction. Again, the random Maxwellain velocities gave higher acceleration. Thus, this distribution was used for further analysis. Plots similar to single and 5 molecules between acceleration and pulse number were generated. Figure 4.17 shows

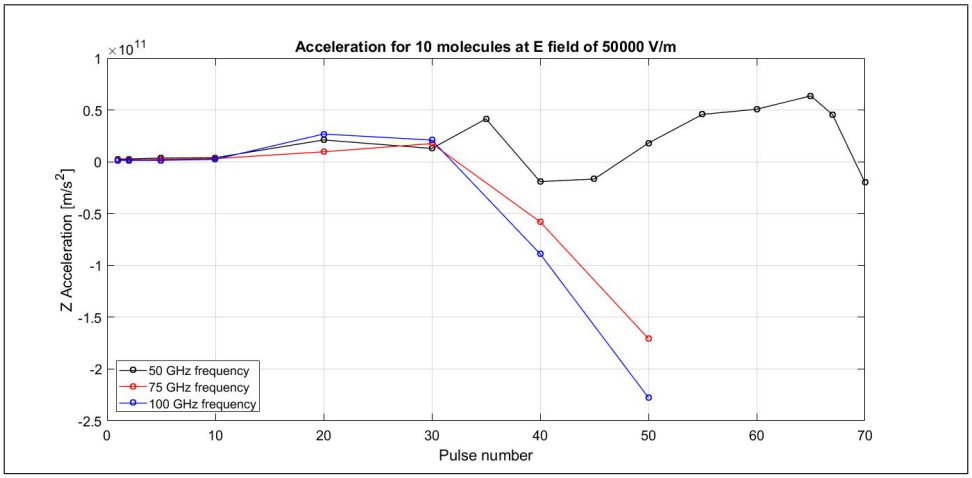

Figure 4.17. Acceleration dependent on the pulse for 10 molecules at 50,000 V/m

the plot of acceleration for 50,000 V/m at 50 GHz, 75 GHz, and 100 GHz. The intermolecular interactions of the 10 molecules had a different effect on acceleration compared to 5 molecules. The acceleration remained in the range of 10^9 m/s^2 up to 30 pulse cycle, independent of the frequency. Thus, for 10 molecules, changing the frequency did not alter the acceleration much initially. For 75 GHz and 100 GHz, the acceleration turned into deceleration when the electric pulse cycle was increased from 30. Whereas the acceleration peaked to 6.361×10^{10} m/s^2 for

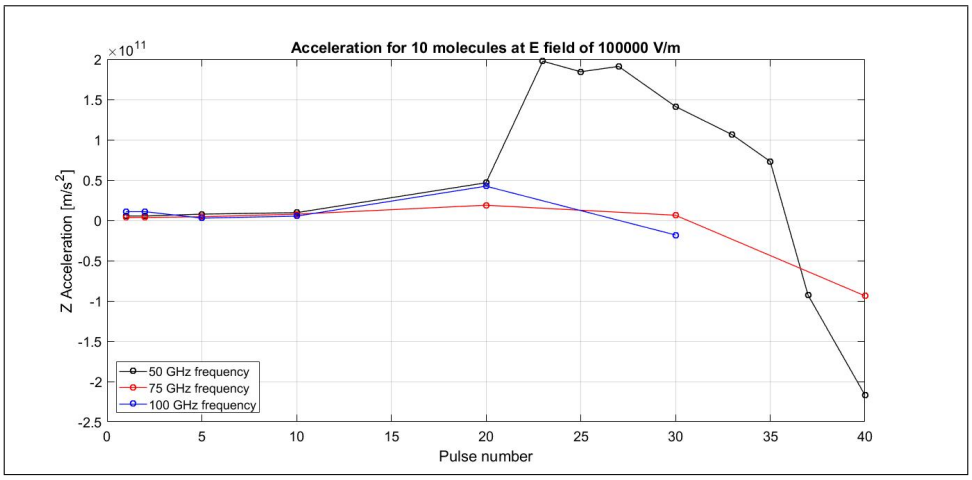

Figure 4.18. Acceleration dependent on the pulse number for 10 molecules at 100,000 V/m

50,000 V/m at 50 GHz when 65 electric pulse cycles were applied. Then, the electric field strength was increased to 100,000 V/m and the acceleration plotted is shown in Figure 4.18. Again the effect of frequency was minimal for lower pulse numbers, but the acceleration peaked when 23 electric pulse cycle of 100,000 V/m were applied at 50 GHz. The maximum acceleration obtained was 1.974×10^{11} m/s^2, higher than the maximum acceleration obtained for 50,000 V/m. Maximum acceleration at each condition is shown in Table 4.6.

Table 4.6. Acceleration comparison from plots for ten molecules

Acceleration [m/s^2]	**Pulse number**	**Electric field** [V/m]	**Frequency** [GHz]
1.974×10^{11}	23	100,000	50
6.361×10^{10}	65	50,000	50
4.240×10^{10}	20	100,000	100
2.677×10^{10}	20	50,000	100
2.106×10^{10}	20	50,000	75
1.877×10^{10}	20	100,000	75

Studying these results for 5 and 10 molecules, it is seen that, although the maximum acceleration decreased with increasing number of molecules, it is still in the range of 10^{11} m/s^2 which is the range of acceleration for current electric propulsion methods. The frequency and pulse cycle required for maximum acceleration are also dependent on the number of molecules. The acceleration peaked at 50 cycles for 5 molecules, whereas it was maximum for 30 cycles for 10 molecules. Thus, so far, no relation can be established between acceleration and pulse number or frequency, but it is very clear that acceleration is increasing with increase in electric field strength. More realistic simulations with even higher number of water molecules can give a clear estimate of the acceleration being produced by Abraham effect.

4.4 12 molecules

So far, the simulation results have shown that acceleration of randomly moving water molecules subjected to single or multiple electric pulses in the x direction and a constant magnetic field in y direction is possible in the z direction. In the simulations done so far, multiple water molecules were all oriented in the same initial position. All the molecules had a zero x and z polarity and a non-zero maximum y polarity obtained by orienting the molecules in the x-y plane in the same fashion separated by some molecular separation distance. To generate a more practical scenario, next the molecules were given random initial orientations.

Consider two molecules with equal-but-opposite polarities cancelling each others' effect. One molecule can have a maximum positive x polarity and another can have a maximum negative x polarity, both with zero y and z polarity. This pair can be possible in two planes, that is the x-y plane and x-z plane. That would result in 4 molecules. Now the same can be true for 4 more molecules cancelling positive and negative y polarities and 4 more cancelling positive and negative z polarities. These would result in a total of 12 molecules with some molecular separation distance between them. A molecular dynamics simulations code was prepared to give these initial orientations to molecules, which would result in a zero initial polarity. All the other initial conditions are listed in Table 4.7.

Table 4.7. Conditions used for generating 12 molecules simulations.

Quantity	Value	Direction
Number of molecules	12	
Electric field	50 kV/m or 100 kV/m	x
Magnetic field	25 T	y
Pressure	4000 Pa	
Temperature	300 K	
Molecular separation	2.3162×10^{-3} m	

Figure 4.19 shows the polarity plot of 12 molecules having random initial orientations and velocities. The total polarity begins with zero in each direction due to the initial orientation. As the simulations advance, there is very little effect on the y polarity but the x polarity increases and the z polarity increases in the negative direction. Again, as the magnetic field is in the y-direction, the polarity of molecules remains unchanged in that direction. The effect of the pulse is seen on all the three polarities. The molecules here are interacting and also aligning under the effect of the electric pulse. There is a single pulse of 100,000 V/m acting at 75 GHz at 35 ps. The total polarity follows the x polarity more or less as that is dominant. Total polarity is changing due to the molecular collisions, orientations, random velocities, and random orientations in all the directions. The cycle of pulses were increased gradually and acceleration was plotted at different electric field strengths and frequencies. The acceleration plots obtained are shown in Figures 4.20 and 4.21.

Figure 4.20 shows the acceleration obtained for 12 molecules at 50,000 V/m. The acceleration

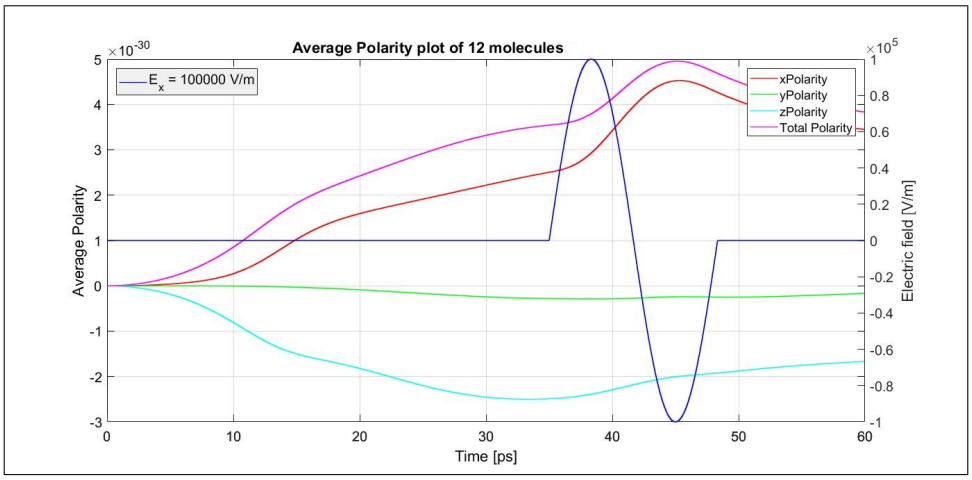

Figure 4.19. Polarity plot for 12 molecules with random initial velocities and orientations

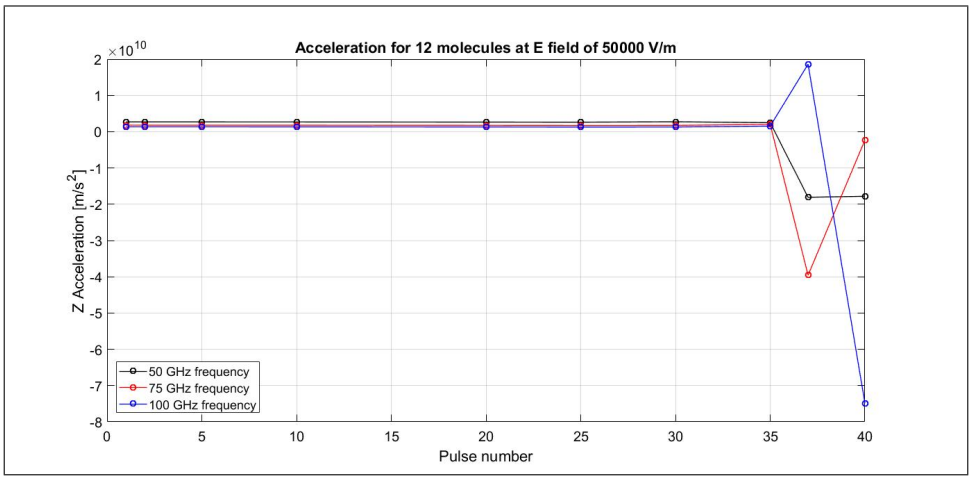

Figure 4.20. Acceleration dependent on the pulse number for 12 molecules at 50,000 V/m

shows little effect of the change in frequency until 35 electric pulse cycles are applied. After that, the acceleration peaks to 1.861×10^{10} m/s^2 for 100 GHz at 37 pulse cycles. Acceleration continuously decreases with the increase in the pulse number for 50 GHz and turns into deceleration at 40 pulse cycles. For 75 GHz, acceleration was maximum for 35 pulse cycles, but still lower than the maximum acceleration at 100 GHz. Thus, 37 electric pulse cycles and a higher frequency of 100 GHz proved beneficial over 75 GHz and 50 GHz. Maximum acceleration for 75 GHz was 2.033×10^9 m/s^2 and for 50 GHz was 2.696×10^9 m/s^2.

In Figure 4.21, again it is seen that higher acceleration is obtained with an electric field strength of 100,000 V/m compared to 50,000 V/m for 12 water molecules. Initially, the acceleration for all the frequencies remained close together up to 35 electric pulses. For 50 GHz, maximum acceleration is 6.575×10^9 m/s^2 with 35 electric pulse cycles, after which it turns into deceleration at 40 electric pulse cycles. The same trend is followed at 100 GHz with a maximum acceleration of 3.021×10^9 m/s^2 at 35 electric pulse cycles. For both frequencies, acceleration

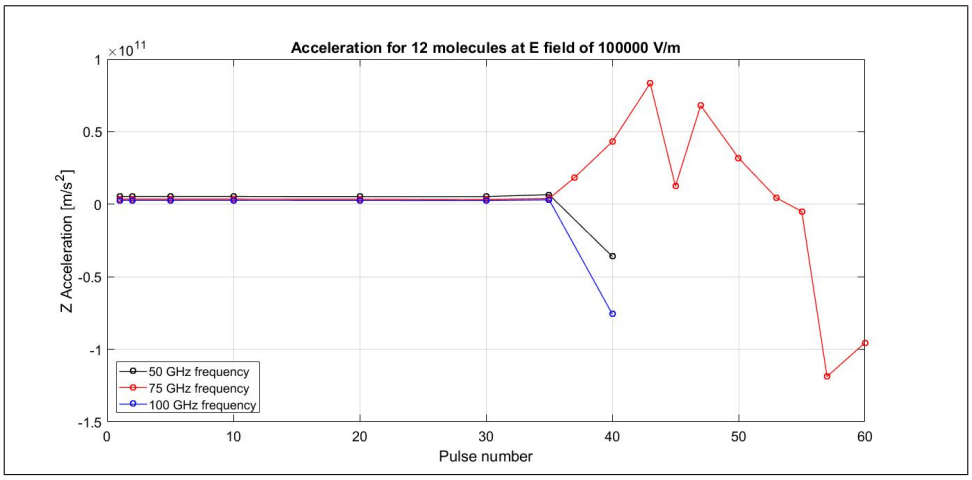

Figure 4.21. Acceleration dependent on the pulse number for 12 molecules at 100,000 V/m

keeps decreasing after a single pulse, but increases at 35 pulses and then turns into deceleration. At 75 GHz though, acceleration kept decreasing after a single pulse up to 30 electric pulses, then started increasing and peaked at 43 and 47 electric pulses. The maximum acceleration obtained is 8.341×10^{10} m/s^2 at 43 electric pulse cycles. Again the maximum acceleration for each case is shown in Table 4.8. The 12-molecule simulations were an important stepping stone for achieving acceleration of molecules with random initial orientations. These results formed the basis for simulating yet higher numbers of molecules.

Table 4.8. Acceleration comparison from plots for 12 molecules

Acceleration [m/s^2]	**Pulse number**	**Electric field** [V/m]	**Frequency** [**GHz**]
8.341×10^{10}	43	100,000	75
1.861×10^{10}	37	50,000	100
6.575×10^{9}	35	100,000	50
3.021×10^{9}	35	100,000	100
2.696×10^{9}	1	50,000	50
2.033×10^{9}	35	50,000	75

4.5 120 Molecules

After successful simulations of 12 molecules with six initial orientations, the molecular dynamics simulations were extended to 120 molecules. All of the 120 molecules had a random initial orientation and a initial total polarity of zero. The acceleration obtained from this case is closest to the result for a real gas. Analysis similar to the previous cases was carried out at 100,000 V/m and frequencies of 50 GHz, 75 GHz, and 100 GHz. All of the initial conditions of the molecules remain the same as 12 molecules with the molecular separation of 4.99×10^{-3} m.

The polarity plot of 120 molecules is shown in Figure 4.22. All the molecules add up to zero initial polarity in all the directions. The nature of the plot is very similar to 12 molecules with the six initial orientations. There is a single electric field pulse of 10,000 V/m at 75 GHz acting at 35 ps. Molecules orient under the effect of the electric pulse as apparent from the polarity plot. The total polarity follows the trend of x polarity again.

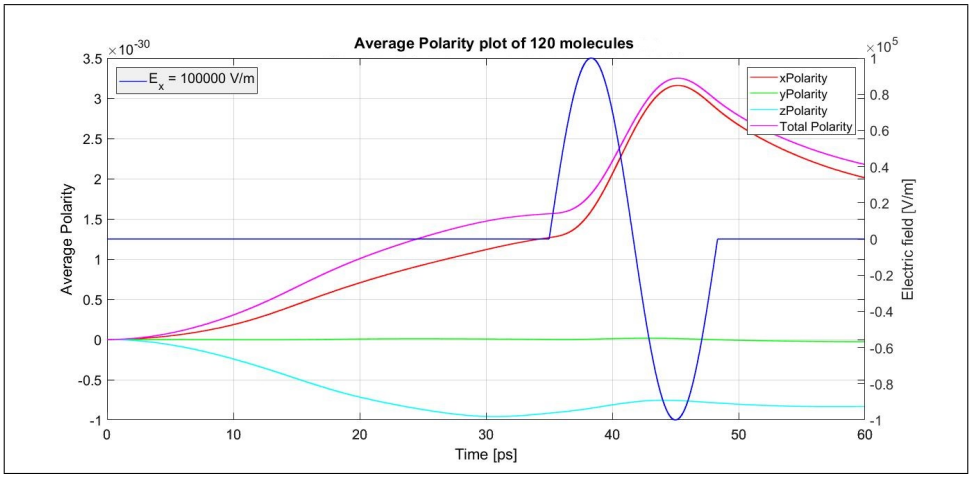

Figure 4.22. Polarity plot for 120 molecules with random initial velocities and orientations

It is clear from the previous sections that acceleration is higher for 100,000 V/m compared to 50,000 V/m. Thus, to save simulation time, results for only 100,000 V/m electric field strength were calculated at three frequencies for 120 molecules. They have random Maxwellian initial velocities. The acceleration-versus-pulse-number plot is shown in figure 4.23. It starts by giving

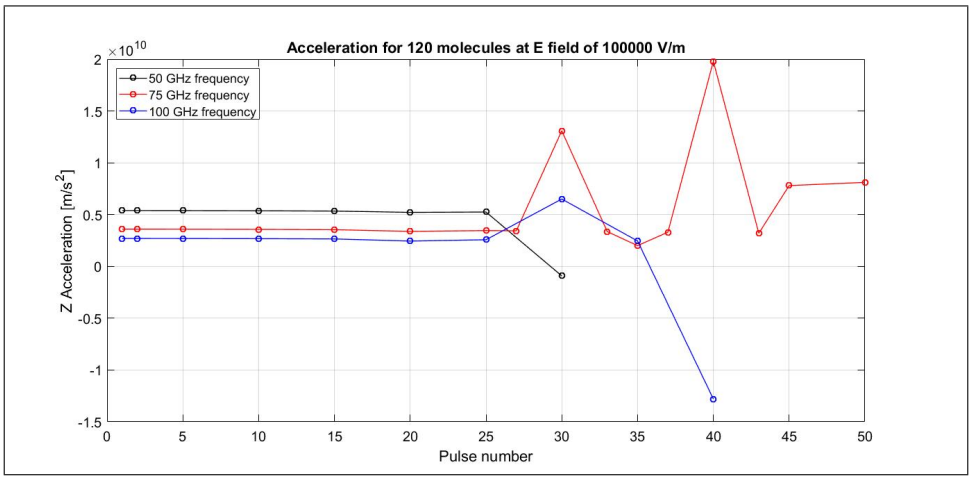

Figure 4.23. Acceleration dependent on the pulse number for 12 molecules at 100,000 V/m

a maximum acceleration for 50 GHz with a single electric field pulse. The acceleration then keeps on decreasing with the increase in the pulse cycles. For 50 GHz, it turns to deceleration at 30 electric pulses. 100 GHz has a maximum acceleration of 6.502×10^9 m/s^2 at 30 electric pulses

and turns into deceleration after that. For 75 GHz, the acceleration peaks at 1.979×10^{10} m/s^2 at 40 electric pulse cycles. Thus, a maximum acceleration of the order of 10^{10} m/s^2 is obtained for 120 molecules having random initial velocities and orientations. This can be the comparison point with current electric propulsion techniques as these simulations are closest to practical experimental conditions.

For gauging the acceleration promised by the simulations, it is compared with the acceleration from current electric propulsion methods. Acceleration from the current electric propulsion techniques with propellants like xenon fall in the range of 10^{11} m/s^2. An accountable fraction of the input energy in the current techniques get converted into the ionization energy to ionize the incoming neutral propellant. Dipole propulsion shown here with molecular dynamics simulations gave accelerations in the range of 10^{10} m/s^2 and even 10^{12} m/s^2 with a non-ionized propellant. To obtain an exhaust velocity in the range of current methods, the acceleration distance required can be calculated. The distance for which the propellant needs to be accelerated for the most realistic case of 120 molecule simulations is calculated by

$$d = \frac{at^2}{2}, \tag{4.4}$$

which can be written as

$$d = \frac{v^2}{2a}, \tag{4.5}$$

where v is the required exhaust velocity and a is the acceleration obtained. It gives a distance of 2.12 cm to obtain an exhaust velocity of 29,000 m/s for an acceleration of 1.979×10^{10} m/s^2. This distance is small, highly feasible and in the range similar to current thrusters. The results obtained successfully established the practicality of the dipole propulsion.

Chapter 5

Conclusion

The current techniques of electric propulsion are characterized by low efficiencies at low specific impulses. Low efficiency of a propulsion system means higher energy losses and lower energy being converted to the kinetic energy of the propellant. The major loss is due to the energy being used for ionization of the propellant. The propellant first needs to be ionized before its acceleration through an electric field in case of electrostatic thrusters or electric and magnetic fields in case of electromagnetic thrusters. If this energy being used for ionization can also be converted to kinetic energy of the propellant, the efficiency of the thruster can be increased.

Abraham solved the system of equations for electrodynamics of moving body and added a new term of force density to them. Suggesting a thruster concept, Cox visualized using that Abraham force acting on a dipole to accelerate it through an electromagnetic force field. He derived a force acting on a dipole that is subjected to perpendicular and varying electric and magnetic fields. The force Cox derived was directly proportional to frequency, dipole moment, and magnetic field strength. Paunescu did first successful molecular dynamics simulations using a steady magnetic field and a high frequency varying electric field in perpendicular directions. The simulations showed that switching on a high frequency electric field aligned and accelerated the molecule in a direction perpendicular to both electric and magnetic fields. The propellants examined were lithium hydride and water. He showed a maximum acceleration in the range of 10^6 m/s^2 with a water molecule. Contri further studied all the possible propellants and advocated the use of water due to its abundant availability and it being a green propellant. Contri compared various initial orientations of a single molecule for maximum acceleration. He then extended the single molecule simulations to 1000 molecule simulations to study the intermolecular effects. This research is built upon this earlier research with the goal of establishing dipole propulsion as a viable electromagnetic propulsion method producing similar acceleration to the current methods but with higher efficiency.

The molecular dynamics simulations of multiple molecules were extended in this thesis. Three molecular forces, the Lorentz force, Coulomb force, and Lennard-Jones force acting between the

atoms and/or the molecules are calculated by the molecular dynamics method. The equations of motion are integrated to find the velocity at next time step using the RATTLE algorithm. Constraint dynamics and periodic boundary condition algorithms were successfully implemented to constrain the bond length of the molecule and to constrain its motion within the simulation volume. The simulation environment consisted of a x-directional sinusoidal electric field and a y-directional constant magnetic field. A single electric field pulse of 21 kV/m at 75 GHz was applied with the magnetic field strength of 25 T. Momentum and polarity were monitored for 1000 ps. Application of the electric pulse showed a momentary change in the polarities indicating alignment of the molecules.

The ultimate goal of the research was to show the acceleration of multiple water molecules subjected to the Abraham force. This goal was realized by calculating the acceleration produced by the Abraham force via molecular dynamics simulations. The acceleration was calculated by comparing the change in z velocity in the presence of an electric pulse and in the absence of one. A steady magnetic field of 25 T in the y-direction remained constant. To establish dipole propulsion as a viable concept, effects of electric field strengths, frequencies, number of pulses, initial velocity, and initial position on the acceleration were studied. Acceleration obtained for multiple molecules having random initial velocities is a breakthrough result of this research. Conditions similar to experimental conditions were simulated. Electric field strengths of 50 kV and 100 kV were used for simulations at 50 GHz, 75 GHz, and 100 GHz. Initial velocities similar for all molecules in all the directions versus randomly generated Maxwellain velocities were simulated. The number of pulses was gradually increased to find the highest acceleration.

For a single water molecule, a maximum acceleration was obtained for a single pulse of 100 kV electric field strength at 50 GHz. For 5 molecules, the randomly generated initial velocities gave an maximum acceleration of 1.011×10^{12} m/s^2 for 50 pulse cycle of 100 kV applied at 50 GHz. This demonstrated that, not only can multiple molecules with random velocities be accelerated by the Abraham force, but that collisions aid in the acceleration process generating a maximum acceleration of the order of 10^{12} m/s^2. When the simulations were extended to 10 water molecules, with random initial velocity, maximum acceleration became 1.974×10^{11} m/s^2 when 25 electric pulse cycle of 100 kV/m were applied at 50 GHz. These simulations had molecules oriented in the same direction initially. 12-molecule simulations were then carried out with six initial orientations. Initial polarity was calculated as 0 as each pair of molecules had equal and opposite values of polarity. Acceleration again was obtained with such initial orientations. The simulations were finally extended to 120 molecules, having random initial velocities and positions. This simulation case had a direct practical application. A propellant in the experiment will enter with random velocities and orientations of molecules. The simulations demonstrated that, if such a propellant is subjected to 40 electric pulse cycles of 100 kV at 75 GHz, it will give an acceleration of 1.979×10^{10} m/s^2.

The molecular dynamics simulations in the research successfully showed acceleration of multiple water molecules subjected to the Abraham force. Also the acceleration obtained from the simulations was comparable with acceleration of current electric propulsion methods using ionized

propellants. There is scope for simulations with even higher number of molecules and monitoring the acceleration produced. 120 molecules can sufficiently gauge the functionality of a real gas, but an even larger number of molecules might shed more light on the intermolecular interactions and effect of the changes in frequencies. The immediate next step can also involve performing an experiment at the optimum conditions obtained from the simulations. An experiment in dipole propulsion could validate the concept and if the acceleration from the experiment is comparable to the simulations' acceleration values, dipole propulsion can replace current propulsion methods having lower efficiency for some missions.

An experimental setup similar to Paunescu's shown in Figure 2.4 can be used to perform such an experiment. Essential experimental hardware include hot plate, pressure transducer, thermocouple, vacuum pump, electric field generators, permanent magnets, and oscilloscopes. However, means to generate higher electric and magnetic fields are required. The number of electric field cycles need to be regulated as well. A mechanism similar to the 'flapper' device can be used to detect acceleration and, once detected, measured by some means. The measured acceleration then needs to be compared with the range of 10^{11} m/s^2 of the current thrusters. The results of the experiments can also validate the simulation results.

Extremely encouraging results for dipole propulsion were obtained from this research. The research showed acceleration of a thermally moving water molecule subjected to the Abraham force. It showed acceleration of multiple molecules with random velocities and orientations. Also, the effect of various electric field strengths, electric field cycles, and frequencies on the acceleration process were examined. Polarity plots showed alignment of the molecules. The simulation results provide all the arguments required to invest the time and money for performing an experiment with dipole propulsion. Acceleration of the current propulsion techniques is in the range of 10^{11} m/s^2 and molecular dynamics simulations of dipole propulsion gave an acceleration in the range of 10^{10} m/s^2 which can be applied over a distance of a few centimeters to obtain an exhaust velocity similar to the current electric propulsion techniques.

Bibliography

[1] Saltzer, C., Craig, R., and Fetheroff, C., "Comparison of Chemical and Electric Propulsion Systems for Interplanetary Travel," *Proceedings of the IRE*, Vol. 48, No. 4, 1960, pp. 465-476.

[2] Bennett, J.,"'Mars Engine' Shatters Records for Ion Propulsion," *Popular Mechanics*, Available: https://www.popularmechanics.com/space/moon-mars/news/a28754/new-ion-thruster-breaks-records-power-thrust/, Accessed: July 16, 2018.

[3] Rumble, J. R., Lide, D. R., and Bruno, T. J., *CRC Handbook of Chemistry and Physics: A Ready-reference Book of Chemical and Physical Data*, Boca Raton: CRC Press, 2018.

[4] Abraham, M., "Zur Elektrodynamik Bewegten Kröper," *Rendiconti del Circolo Matematico di Palermo*, 17 Jan. 1909, pp. 1-28.

[5] Abraham, M., "On the Electrodynamics of Moving Bodies," *Neo–classical–physics.info* Available: http://www.neo–classical–physics.info/uploads/3/0/6/5/3065888/abraham_–_ed_of_moving_bodies.pdf, Translated by: Delphenich, Accessed: June 13, 2017.

[6] Penfield, P., and Haus, H. A., *Electrodynamics of Moving Media*, *The MIT Press*, Chapter 3, 1967.

[7] Walker, G. B., and Walker, G., "Mechanical Forces of Electromagnetic Origin," Vol. 263, p. 401, Sept. 30, 1976.

[8] Walker, G. R., Lahoz, D. G., and Walker, G.,"Measurement of the Abraham Force in a Barium Titanate Specimen," *Canadian Journal of Physics*, Vol. 53, pp. 2577–2586, Dec 1975.

[9] Cox, J. E., "Electromagnetic Propulsion Without Ionization," AIAA Paper 80–1235, July 1980.

[10] Cox, J. E., "Shuttle Propulsion Using Electromagnetic Force Fields," AIAA Paper 81-1535, July 1981.

[11] Cox, J. E., "Electromagnetic Propulsion Without Ionization," *Journal of Spacecraft and Rockets*, Vol. 18, pp. 449–456, Sept.-Oct. 1981.

[12] Micci, M. M., "Analysis of Electromagnetic Propulsion of Nonionized Dipole Gases," *Journal of Spacecraft and Rockets*, Vol. 22, No. 4, pp. 469–473, July–August 1985.

[13] Paunescu, C., and Micci, M. M., "Investigation of Electromagnetic Acceleration of Nonionized Gases," M.S. Thesis, Pennsylvania State University, 2009.

[14] Contri, J., "Molecular Dynamics Simulation and Investigation of Electric Fields for the Use of Nonionozed Dipole Gases in Electromagnetic Propulsion," B.S. Thesis, Pennsylvania State University, 2017.

[15] Alder, B. J., Wainwright, T. E., "Studies in Molecular Dynamics. I. General Method," *J. Chem. Phys*, Vol. 31, No. 2, pp. 459, 1959.

[16] Bandel, H. W., and MacDonald, A. D., "Microwave Breakdown in Air Plus H_2O," *Journal of Applied Physics*, Vol. 41, No. 7, pp. 2903-2904, June 1970.

[17] Sodawala, S., Contri, J., and Micci, M., "Investigation of Electric Fields for Electromagnetic Propulsion using Nonionized Dipole Gases," *IEPC*, Oct 2017, Available: https://iepc2017.org/sites/default/files/speaker–papers/paper.pdfp=DevEx.LB.1,5502.1.

[18] Hansen, J., Schrøder, T., and Dyre, J., "Simplistic Coulomb Forces in Molecular Dynamics: Comparing the Wolf and Shifted-Force Approximations," *The Journal of Physical Chemistry B*, Vol. 116, No. 19, 2012, pp. 5738-5743.

[19] Fanourgakis, G.,"An Extension of Wolf's Method for the Treatment of Electrostatic Interactions: Application to Liquid Water and Aqueous Solutions," *The Journal of Physical Chemistry B*, Vol. 119, No. 5, pp. 1974-1985, January 2015.

[20] Frenkel, D.,and Smit, B., "Understanding Molecular Simulations: From Algorithms to Applications," Edition 2, Elsevier Science, 2001.

[21] Andersen, H.C., "RATTLE: A 'Velocity' Version of the SHAKE Algorithm for Molecular Dynamics Calculations," *Journal of Computational Physics*, Vol. 52, pp. 24-34, 1983.

[22] Ryckaert, J.–P., Ciccotti, G., Berendsen, H.J.C., "Numerical Integration of the Cartesian Equations of Motion of a System with Constraints: Molecular Dynamics of n-Alkanes," *Journal of Computational Physics*, Vol. 23, No. 3, pp. 327-341, 1977.